CHARACTERIZATION OF ROTATING DETONATION ENGINE EXHAUST THROUGH NOZZLE GUIDE VANES

THESIS

Nick D. DeBarmore, Second Lieutenant, USAF

AFIT/GAE/ENY/13-M09

DEPARTMENT OF THE AIR FORCE
AIR UNIVERSITY

AIR FORCE INSTITUTE OF TECHNOLOGY

Wright-Patterson Air Force Base, Ohio

AFIT/GAE/ENY/13-M09

CHARACTERIZATION OF ROTATING DETONATION ENGINE EXHAUST THROUGH NOZZLE GUIDE VANES

THESIS

Presented to the Faculty

Department of Aeronautics and Astronautics

Graduate School of Engineering and Management

Air Force Institute of Technology

Air University

Air Education and Training Command

in Partial Fulfillment of the Requirements for the

Degree of Master of Science in Aeronautical Engineering

Nick D. DeBarmore, B.S.

Second Lieutenant, USAF

March 2013

AFIT/GAE/ENY/13-M09

CHARACTERIZATION OF ROTATING DETONATION ENGINE EXHAUST THROUGH NOZZLE GUIDE VANES

Nick D. DeBarmore, B.S.
Second Lieutenant, USAF

Approved:

Paul I. King, PhD (Chairman)	Date
Frederick R. Schauer, PhD (Member)	Date
Maj Jay Rutledge, PhD (Member)	Date

Abstract

A Rotating Detonation Engine (RDE) has higher thermal efficiencies in comparison to its traditional gas turbine counterparts. Thus, as budgets decrease and fuel costs increase, RDEs have become a research focus for the United States Air Force. An integration assembly for attaching the first Nozzle Guide Vane (NGV) section from a T63 gas turbine engine to a 6 inch diameter RDE was designed and built for this study. Pressure, temperature, and unsteadiness measurements were completed in this study to characterize the exhaust flow of the RDE through the NGVs. The experiment found that stagnation pressure dropped an average of 4% through the NGVs, and that unsteadiness as a measurement of dynamic pressure trace peak height was attenuated by a mean of 60% across the NGVs. Additionally, the study found the flow angle of the NGV exhaust to be between 40° and 55°. Finally, the study found that the RDE exhaust flow was approximately 2250 °R before entering the NGVs.

Table of Contents

Page

List of Figures

Figure Page

List of Symbols

Symbol	Definition
η	Thermal Efficiency
γ	Specific Heat Ratio
ϕ	Equivalence Ratio
$\dot{m}$	Mass Flow (lbm/s) [lbm/m]
P	Pressure (psi)
T	Temperature (R) [K]
V	Velocity (m/s)

Subscripts

0	initial
B	Brayton
c	Corrected
CJ	Chapman-Jouguet
H	Humphrey
t	true

List of Acronyms

Acronym	Definition
AFRL	Air Force Research Laboratories
CTAP	Capillary Time Averaged Pressure
DDT	Deflagration to Detonation Transition
DoD	Department of Defense
DERF	Detonation Engine Research Facility
FFT	Fast Fourier Transform
CEA	NASA's Chemical Equilibrium with Applications program
NRL	Naval Research Laboratories
NGV	Nozzle Guide Vane
PDE	Pulse Detonation Engine
RDE	Rotating Detonation Engine
USAF	United States Air Force
ZND	Zeldovich-von Neumann-Döring

CHARACTERIZATION OF ROTATING DETONATION ENGINE EXHAUST THROUGH NOZZLE GUIDE VANES

I. Introduction

CLIMBING fuel prices coupled with Department of Defense (DoD) budget cuts emphasize the necessity for decreased fuel consumption. In response, the United States Air Force (USAF) is supporting research to increase efficiency in aircraft engines.

A major focus for increasing engine efficiency lies in the combustion process. Traditional gas turbine engine combustors operate with an approximate constant pressure deflagration process. Detonation engines have potentially 20% higher propulsive efficiencies than their traditional deflagration counterparts due to the detonation constant volume pressure gain process [1].

1.1 Past Research

The concept of a rotating detonation engine (RDE) is not new. In the 1960s, Voitsekhovskii [2] of the Lavrentyev Institute of Hydrodynamics of the Russian Academy of Sciences investigated detonation waves in gases. In his research, which involved a transverse wave rotating in a circular channel, he characterized the detonation wave structure through luminosity fields, location of shocks at the detonation front, and pressure-profile measurements. Voisekhovskii's [2] research establishes a foundation for modern RDE research. This detonation wave structure matches structures seen in later RDE research by F.A. Bykovskii [3] in 2006 .

Bykhovskii [3] demonstrated the possibility of a continuous transverse wave in a correctly sized detonation channel. Furthermore, he found that this transverse detonation

wave is sustainable via a well-mixed radial injection system. Given proper mixing, the detonation wave velocity and structure was stable in wide ranges of propellant components.

1.2 Engine Efficiency

Deflagration engines and detonation engines differ in efficiency because deflagration combustion is a constant pressure process, while detonation is a constant volume process. The ideal Brayton cycle describes the efficiency of deflagration engines with a constant pressure combustion process. In the Brayton cycle, efficiency (η_B) is a function of the ratio of temperatures before (T_0) and after (T_1) isentropic compression, shown in Eq. 1.1 [4].

$$\eta_B = 1 - \frac{T_0}{T_1} \tag{1.1}$$

Alternatively, the Humphrey cycle models the constant volume combustion process of a detonation engine. The Humphrey cycle is a function of both the ratio of temperatures before (T_1) and after (T_2) combustion as well as the ratio of temperatures before (T_0) and after (T_1) isentropic compression, shown in Eq. 1.2 [4]. As such, the efficiency (η_H) of a detonation combustion process is generally higher than that of a deflagration combustion process. Figure 1.1 shows a comparison of the ideal Brayton cycle and the Humphrey cycle.

$$\eta_H = 1 - \frac{T_0}{T_1}\gamma \left[\frac{\left(\frac{T_2}{T_1}\right)^{\frac{1}{\gamma}} - 1}{\frac{T_2}{T_1} - 1} \right] \tag{1.2}$$

1.3 Current Research Objectives

The objective of this research was to determine the flow characteristics of exhaust from an RDE over NGVs. Specifically, the objective was to integrate an NGV section of a T63 gas turbine engine into the exhaust flow of an RDE. Desired flow characteristics include stagnation pressure and unsteadiness upstream and downstream of the NGV section and

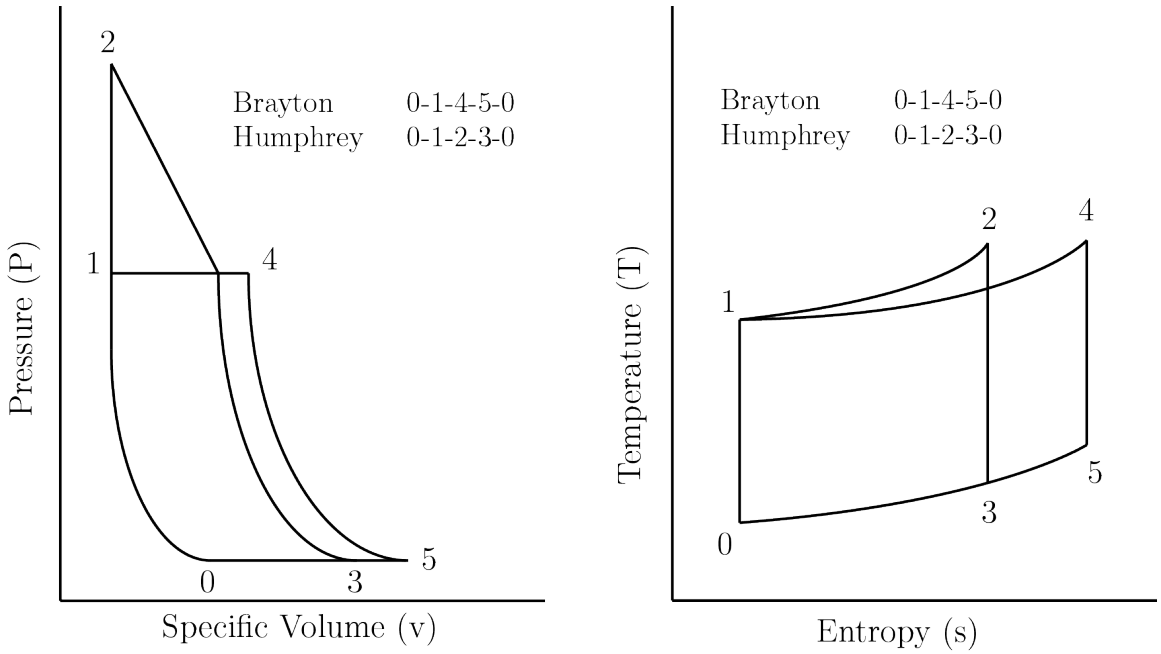

Figure 1.1. P-v and T-s diagrams for ideal Brayton and Humphrey cycles

flow angle in the NGV exhaust. This integration and characterization is a crucial early step in the development of RDEs for practical use in operational aircraft.

1.4 Chapter Preview

Chapter 2 includes a literature review of detonation theory, descriptions of pulse detonation engines (PDE)s and RDEs, and a closer look at previous computational and experimental RDE research. Chapter 3 describes the methodology of this study, including a facility description, the integration design, instrumentation, and data reduction techniques. Chapter 4 provides a discussion of the results from this experiment. Finally, conclusions and recommendations for future research are presented in Chapter 5.

II. Literature Review

EARLY detonation research focused on modeling a detonation wave in one dimension. Observation and measurement of rapid combustion became possible with the development of diagnostic tools at the close of the 19th century. Mallard and Le Châtelier [5] observed Deflagration to Detonation Transition (DDT) with a drum camera in 1883 and deduced that the adiabatic compression wave at the detonation front initiates the chemical reactions.

At the turn of the century Chapman [6] and Jouguet [7] independently postulated that the detonation velocity for a given explosive mixture is that velocity which results in minimum entropy and a supersonic condition upstream of the detonation with an assumption of an infinitely thin reaction zone. This velocity, V_{CJ}, corresponds to the minimum velocity at which detonation will occur. This velocity was supposedly the lowest of a continuous spectrum of possible detonation velocities, however this was disproved with further research. In the 1940s, Zeldovich [8] described the previously mentioned detonation model of a chemical reaction zone following a shock front, which is now known as the Zeldovich-von Neumann-Döring (ZND) model. Zeldovich [8] created a physical model that included heat and momentum losses as well as a finite reaction zone to show that the detonation velocity is less than the equilibrium V_{CJ}. He also determined that V_{CJ} is the detonation equilibrium velocity, with higher detonation velocities only possible for certain reactions. This fundamental one-dimensional model was an early milestone in detonation research and is still used in detonation research to this day.

2.1 Detonation Theory

Deflagration and detonation engines vary in efficiencies because of the difference in their reaction scheme. A combustion wave consumes reactants and creates products,

releasing energy from the chemical bonds of the reactants as it propagates away from the ignition source. In a deflagration wave, reactants combust at subsonic flame speeds which allows downstream disturbances to propagate upstream and affect unburned reactants. Deflagration waves are expansion waves characterized by a pressure decrease across the reaction front.

In contrast, a detonation wave propagates away from the ignition source at sonic flame speeds and is coupled with a shock wave. The shock wave prevents downstream disturbances from affecting upstream unburned reactants. Across the shock, pressure and temperature increase abruptly. The detonation wave is a compression wave and thus density also increases abruptly across the shock. A detonation wave can be considered a deflagration wave coupled with a compression shock wave where ignition of reactants is due to adiabatic compression at the leading shock. The detonation wave propagates forward due to the auto-igniting shock front and a rapid pressure drop in the reaction zone followed by expansion waves.

2.2 Pulsed and Rotating Detonation Engines

Conventional gas turbine engines are subject to poor efficiency, complicated moving parts, and constant pressure combustion. A Pulse Detonation Engine (PDE) combusts a fuel-oxidizer mixture via detonation rather than the traditional gas turbine combustion method of deflagration. It follows that a PDE utilizes the higher efficiency of the Humphrey cycle and constant volume pressure gain combustion. Thus, there is interest in the integration of PDEs as combustors for aircraft engines.

However, PDEs are limited by cycle frequencies of about 100 Hz which create substantially unsteady exhaust. The cycle frequency limitation is due to the fact that a PDE has a non-continuous cycle of fill, fire, and purge, shown in Fig. 2.1, that requires a moving valve structure and repeated ignition. This inherent unsteadiness makes for difficult integration of downstream turbomachinery. PDEs are also limited by the need for a long combustion tube section to allow the deflagration wave to reach supersonic speeds and

transition to a detonation wave. This phenomenon is called deflagration to detonation transition (DDT), and is due to the fact that a self-propagating deflagration is naturally unstable and will accelerate continuously after ignition. Lee [5] states that the deflagration wave will eventually reach sonic velocities and transition to a detonation wave.

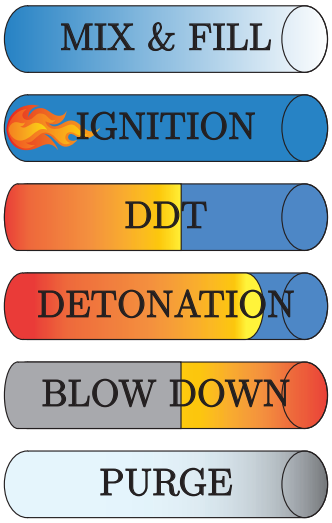

Figure 2.1. PDE combustion process

The RDE removes the size limits of the PDE by forming the combustion section into an annular chamber to minimize the size of the combustor. A deflagration is initiated by a high-energy pre-detonation impulse and transitions to a detonation wave that travels around the annulus at frequencies ranging from 2-3 kHz for a 6 inch diameter rig as seen in Shank's [9] research. The detonation wave eventually reaches a steady state during which exhaust expands axially out of the annulus while fresh reactants from a pressurized chamber fill in behind the detonation front, as seen in Fig. 2.2. Thus, the favorable PDE pressure gain combustion process is preserved, but there are no moving parts and the design is more compact. Furthermore, the RDE has a quasi-steady exhaust due to its continuous cycle. This allows for the integration of downstream turbomachinery.

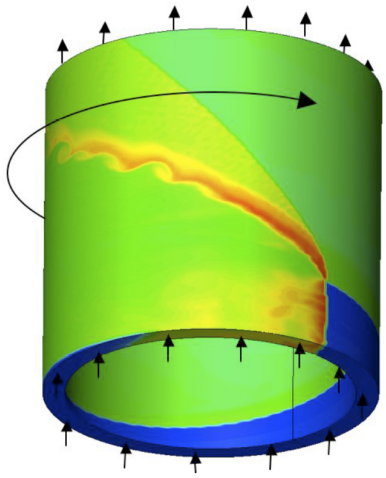

Figure 2.2. RDE with detonation wave [1]

2.3 Computational RDE Research

Researchers [10] at the Naval Research Laboratories (NRL) have studied the detonation flow in RDEs with an ideal premixed injection system. For a study of the detonation wave structure, they used a computational RDE model with annulus geometry of 14 cm and 16 cm inner and outer diameters, respectively. The ratio of inlet nozzle throat area to the wall was 0.2, and the annulus axial length was 17.7 cm. Flow conditions consisted of a stoichiometric hydrogen-air mixture, 10 atm pressurized injection, 300 K stagnation temperature, and ambient back pressure of 1 atm. The model showed that radial flow variation is minimal compared to the axial and azimuthal dimensions. This allowed the researchers to unwrap the RDE for a two dimensional model. Figure 2.3 shows the visualization of the ideal RDE detonation structure. Notable features include the detonation wave (A), oblique shock wave(B), mixing region between old and new detonation products (C), fresh propellant (D), the deflagration where fresh propellant meets hot products (E), and a secondary shock wave (F).

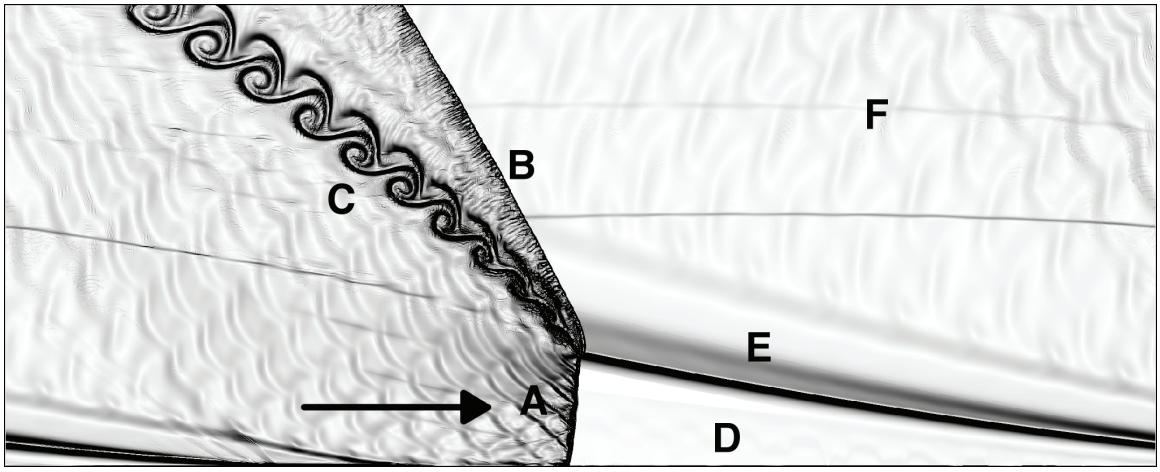

Figure 2.3. Detonation wave structure in an RDE [10]

Before integrating turbomachinery into the exhaust of an RDE, it is be prudent to characterize the RDE exit flow. Kailasanath and Schwer [10] at the NRL address this topic from a computational standpoint. Figure 2.4 shows the pressure, temperature, and velocity of the RDE exit flow compared to the same properties of the inlet flow. The NRL analysis indicates pressure and temperature are an order of magnitude lower in the exhaust plane than in the detonation plane. The research also shows an attenuation of the swirl created by the transverse motion of the detonation wave around the annulus. This decrease in azimuthal velocity between the inlet and outlet is important for exhaust integration into turbines which traditionally experience approximately axial flow.

2.4 Recent RDE Research at AFRL

Research into RDEs at the Air Force Research Laboratories (AFRL) is ongoing. Previous to this study, Shank [9] designed an RDE with a focus on modularity to act as a flexible platform for future RDE research. His design was used for this study. The baseline geometry of his design was a 5.46 in outer diameter center body with a detonation channel width of 0.3 in. The fuel plate thickness and fuel spacer height were 0.5 in and

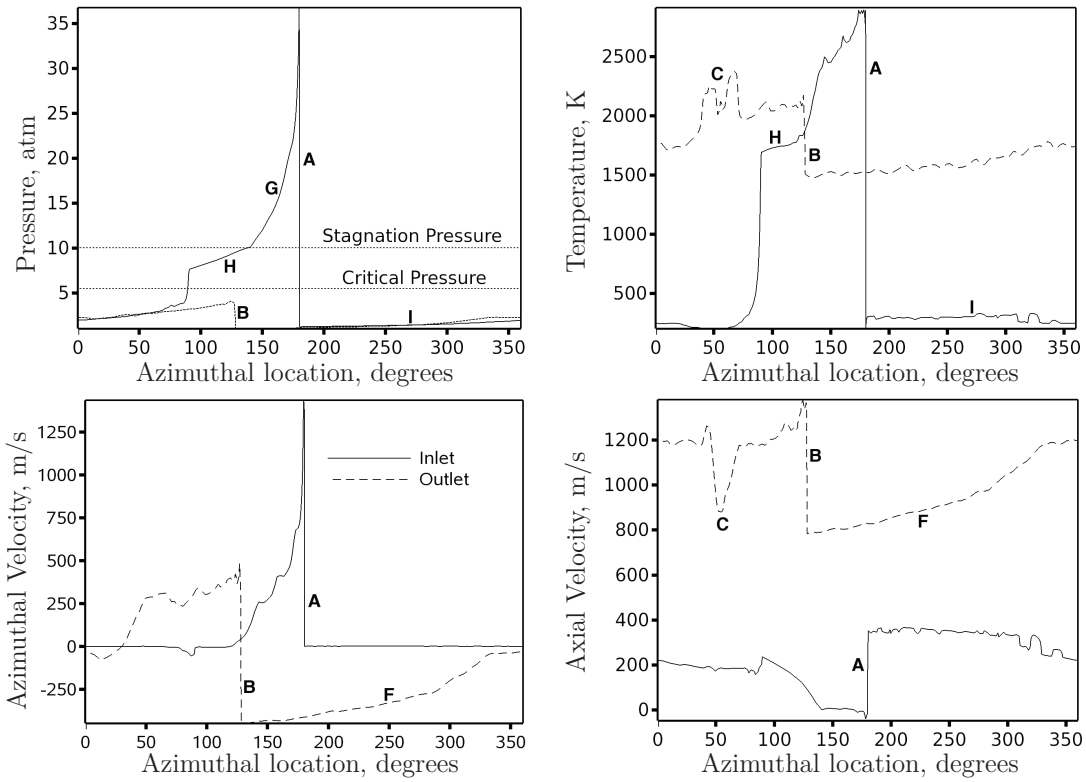

Figure 2.4. Inlet and outlet conditions of a computationally modeled RDE [10]

1.125 in, respectively, and resulted in a 0.125 in jet slot. The fuel plate employed a series of 80, 0.1 in diameter holes arranged on a 5.96 in diameter circle. The design allows for adjustments to oxidizer type, oxidizer injection geometry, fuel type, fuel injection geometry, and detonation channel width. Shank [9] also investigated the operational space of the design and found a linear lower operational boundary between equivalence ratio (ϕ) and fuel mass flow rate ($\dot{m}_{fuel}$) where the minimum equivalence ratio for detonation was 0.94, shown in Fig. 2.5. Shank's [9] research also determined that average detonation velocity was less than V_{CJ}, and postulated that this is likely due to losses and irregularities in the detonation channel that cause reflecting shocks in the opposite direction of the detonation.

Prior to the modular RDE development, Russo [11] modified a 3 in diameter RDE designed for ethylene and oxygen to use with hydrogen and air. The study also involved

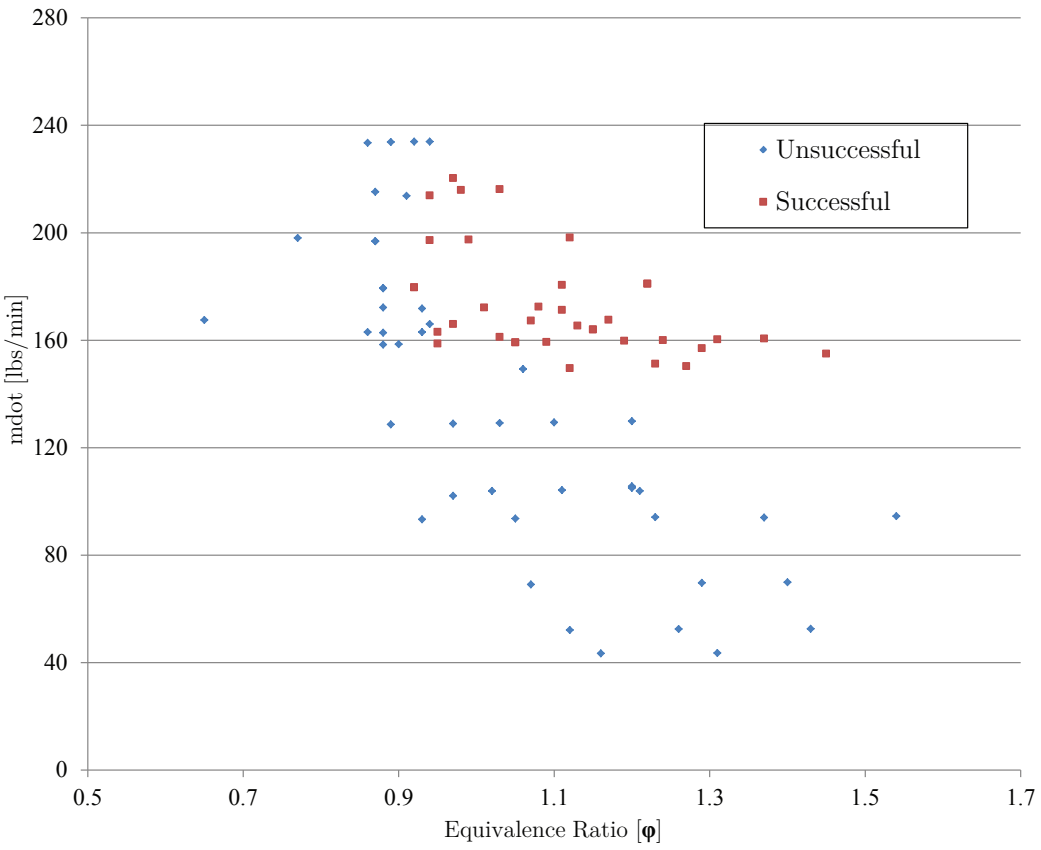

Figure 2.5. Operational space for an RDE run on hydrogen and air [9]

mapping the operational space for hydrogen-enriched air (23% O_2) and hydrogen-standard air (21% O_2) combustion, shown in Fig. 2.6. Individual tests were considered successful if the detonation duration was a full second and if the test point could be repeated three successive times. Russo determined an operational lower limit at total mass flows of about 25 lbm/min for hydrogen-standard air and a linear boundary relationship between total mass flow and equivalence ratio for hydrogen-enriched air. Finally, Russo [11] wrote and validated a time-of-flight code to determine wave speed data from individual RDE tests. Russo's code determines a moving average of instantaneous dynamic pressure data and searches for peaks in pressure at least one standard deviation above the mean. The time between each pressure peak is used in conjunction with the detonation channel circumference to calculate

detonation wave speed [11]. Russo's time-of-flight code was used for data analysis in this research.

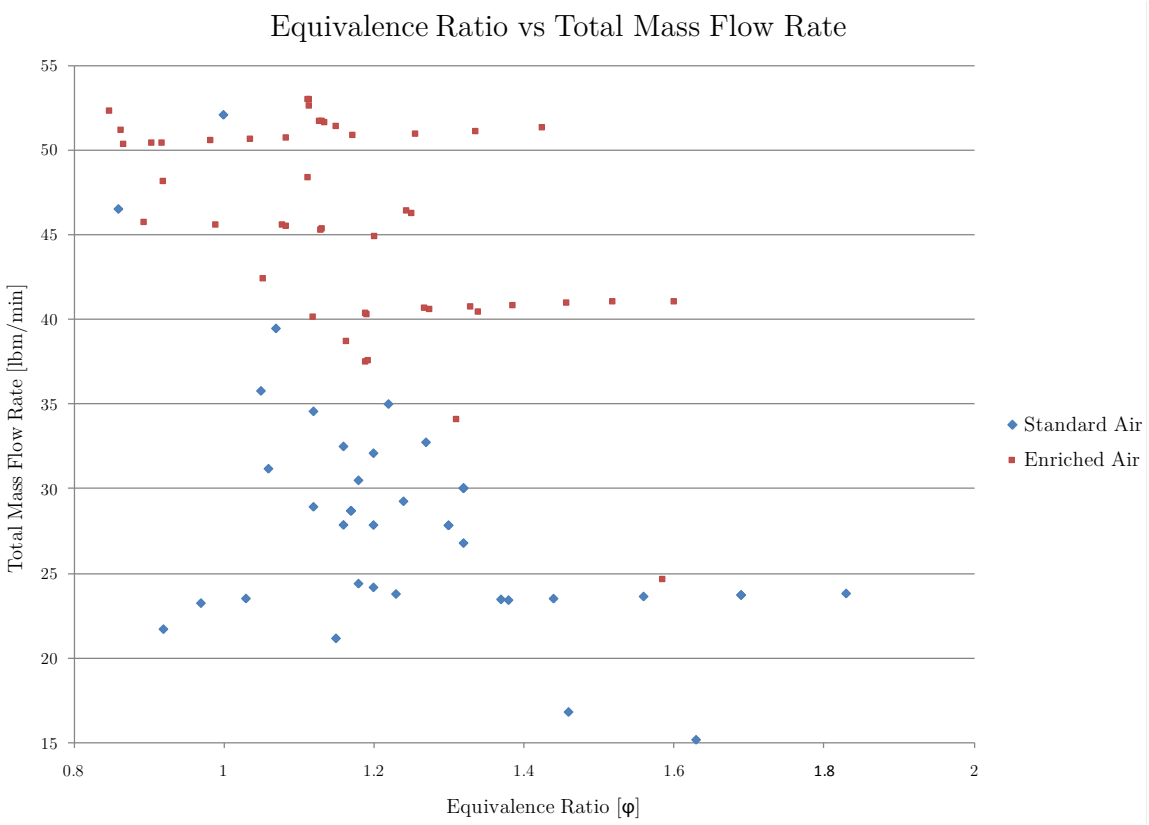

Figure 2.6. Equivalence ratio and total mass flow rate for enriched air and full length standard air runs [11]

Tellefsen [12] engaged in the first-ever RDE-axial turbine testing at AFRL in 2012. Addition of a nozzle increased the operational space of the RDE by allowing lower equivalence ratios at given mass flow rates. This finding shows that placement of turbomachinery behind an RDE benefits RDE operation through backpressure. Tellefsen [12] placed the turbine components of a JetCat P-200 into the exhaust flow of a 3 in diameter RDE and found that while the turbine pressure and RPM data showed unsteadiness, the compressor mass flows and pressure data was near steady state for run times of one second.

His turbine testing ended in a catastrophic failure in which the shaft ruptured near the turbine wheel and the turbine blades sheared from the turbine wheel. This failure was due to operation at high angular speeds of 112,000 RPM and possibly thermal creep of the turbine blades. Tellefsen's [12] research is useful to this study because it gives insight to the possibility of driving a turbine via RDE exhaust.

Recent research at AFRL also includes RDE flowfield characterization by Naples [13] utilizing high speed video of chemiluminescence on a different RDE rig but with the same dimensions as that of Shank [9]. Naples [13] replaced the steel tube outer body with a quartz tube for visual access to the transverse detonation wave. By unwrapping the RDE in a fashion similar to that of the previous computational researchers Kalaisanath and Schwer [10], Naples was able to create a two dimensional view of an entire annulus section by combining multiple frames from high speed video. The detonation wave structure created by averaged light intensity is shown in Fig. 2.7. The study determined the basic flow structure dimensions from chemiluminescence as a basis for validation of RDE models. However, the flow structure dimensions varied significantly and future work is needed to determine the causes of these variations. Naples' [13] visual characterization of the RDE exhaust is useful to this study because it increases insight into the exhaust flow structure encountered by the NGVs.

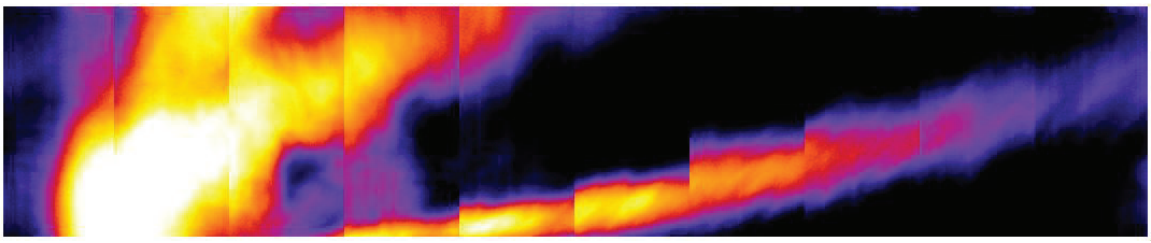

Figure 2.7. Two dimensional RDE average light intensity for 1.55 kg/s [13]

III. Methodology

3.1 Facility

This study was conducted at the Detonation Engine Research Facility (DERF) in building 71A, D-Bay, at Wright-Patterson Air Force Base, Ohio. D-Bay is a component of the AFRL Propulsion Directorate, Turbine Engine Division, Combustion Branch (AFRL/RQTC). The D-Bay facility includes a 748,670 ft^3 test cell encased in 2 ft of reinforced concrete. Inside the test cell is the table to which the RDE is mounted. Additionally, a control room isolated from the test cell contains all the hardware necessary to remotely operate and observe experiments in the test cell. The control room has a control panel made up of physical switches for power supply and fuel, oxidizer, and ignition valves. Physical control over these parameters allows the operator to disable system power and prevent the RDE from firing despite any commands from the control computer. The control computer, which is also in the control room, contains *Labview*® software for controlling the experiment. *Labview*®monitors low speed data such as the fuel and air pressure (upstream and downstream of the sonic nozzles) as well as high speed data up to 5 MHz such as instantaneous pressures in the detonation channel. Figure 3.1 details the fuel and air delivery system for the RDE setup at D-Bay. Nitrogen is used for dome pressure on the dome-loaded pressure regulators. Hydrogen and air pass through the pressure regulators, sonic nozzles which set the mass flow, and finally fast-actuation air-driven solenoid valves to the RDE. Pre-detonation ignition uses pure oxygen and hydrogen to start the detonation in the RDE.

3.2 T63 Engine

The Allison Model M250, with the military designation of T63, is a 250 Bhp gas turbine engine built with 1960s technology, shown in Fig. 3.2. This highly successful engine has been used in both helicopters and turboprop airplanes, including the Bell Jet Ranger.

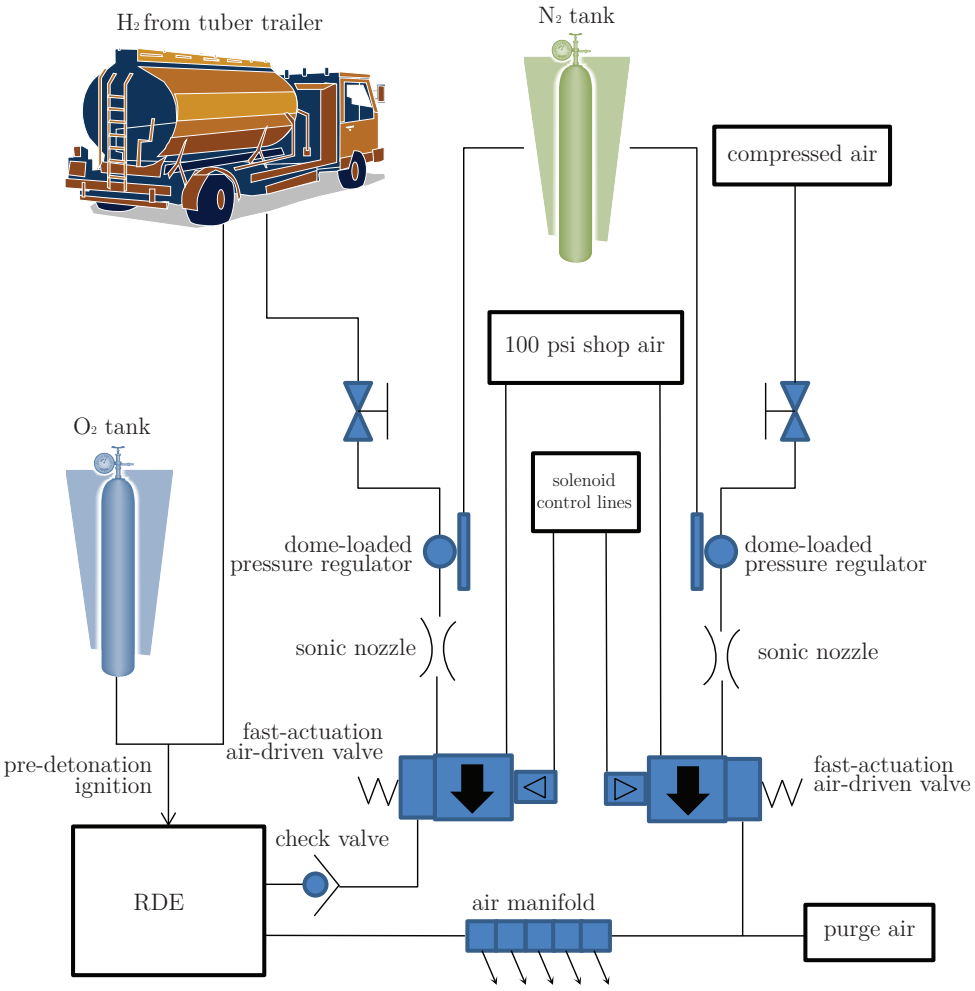

Figure 3.1. Fuel and air delivery system for an RDE at D-Bay

The T63 is a twin spool engine that utilizes a six stage axial compressor with rear stage centrifugal impeller, a single can-type reverse flow combustion chamber, two stages of gas producer axial turbine, and two stages of power output axial turbine. Figure 3.3 provides a top down view of the T63 gas turbine engine where the NGV assembly used in this experiment is visible.

The turbine section of the T63 has 25 uncooled 1st stage NGVs that are designed to withstand temperatures up to 2000 °R [14]. Figure 3.4 shows images of the T63 NGV

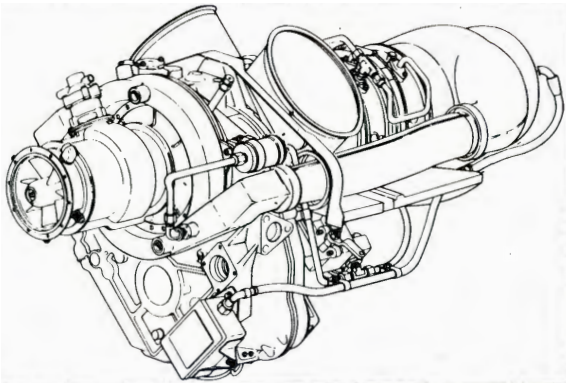

Figure 3.2. T63 gas turbine engine

Figure 3.3. Location of NGV assembly

components. The 1st stage nozzle is a stainless steel investment casting of vanes and inner and outer supporting bands. The stainless steel heat shield, visible in Fig. 3.4b, shields the five support struts within the turbine assembly and directs the exhaust gases from the combustion liner into the NGVs. The heat shield also protects the oil sump in the center of the gas producer turbine. This project used the original T63 assembly hardware to allow for modular continuity with T63 parts and placed the RDE exhaust in the same flow path as the T63 combustor exhaust. No T63 engine components were modified for the design of this study to allow for future developments of full integration of the RDE into the engine.

3.3 Design

An integration assembly was designed to duct the exhaust flow of the RDE into the NGVs with minimal discontinuities. The RDE design developed by Shank [9] was used

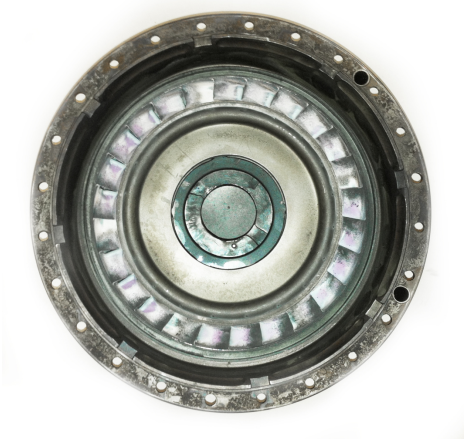

(a) NGV Assembly (top view)

(b) NGV assembly (bottom - heat shield visible)

(c) T63 nozzle guide vanes

Figure 3.4. NGV assembly components

for this study with a few minor modifications. The lowest equivalence ratio possible was desired for this study to reduce exhaust temperature, as the T63 components were not built to withstand RDE exhaust temperatures at high equivalence ratios, which can be on the order of 3700 °R. However, as seen in Shank's [9] research, minimum equivalence ratios for this RDE are about 0.9. Ongoing research at AFRL has indicated that a smaller oxidizer gap in

the RDE promotes better mixing and expands the RDE operating area to lower equivalence ratios. Thus, Shank's [9] 1.125 in oxidizer gap was replaced with a 1.062 in gap, which is shown in Fig. 3.5. Equivalence ratios for this study ranged from 0.39 to 0.61.

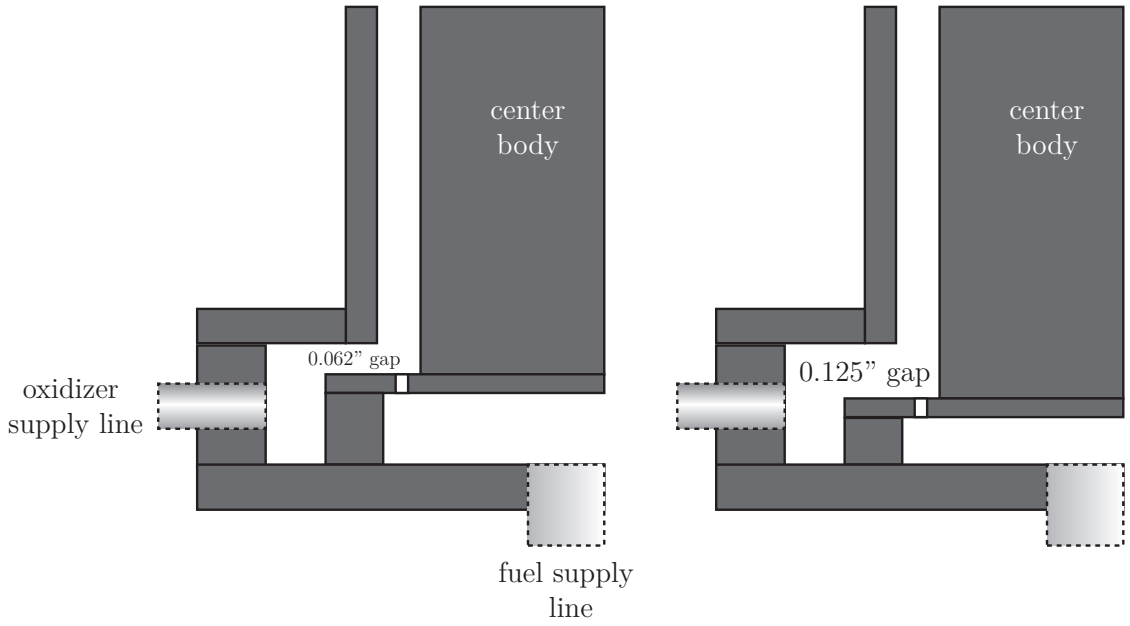

Figure 3.5. Change to fuel spacer plate to allow for better mixing

Furthermore, the design assembly for this study adds backpressure by placing components in the RDE exhaust, and ongoing research at AFRL [12] has also shown that this allows operation at lower equivalence ratios. Additionally, a flange ring was welded to the top of the RDE outer body as a mounting platform for downstream components. The designed integration assembly includes an adapter flange, an extended RDE center body, and inner/outer bodies for the NGV exhaust. The complete assembly is shown in Figure 3.6, and each subsequent part is explained next. Detailed technical drawings of these parts are provided in Appendix A.

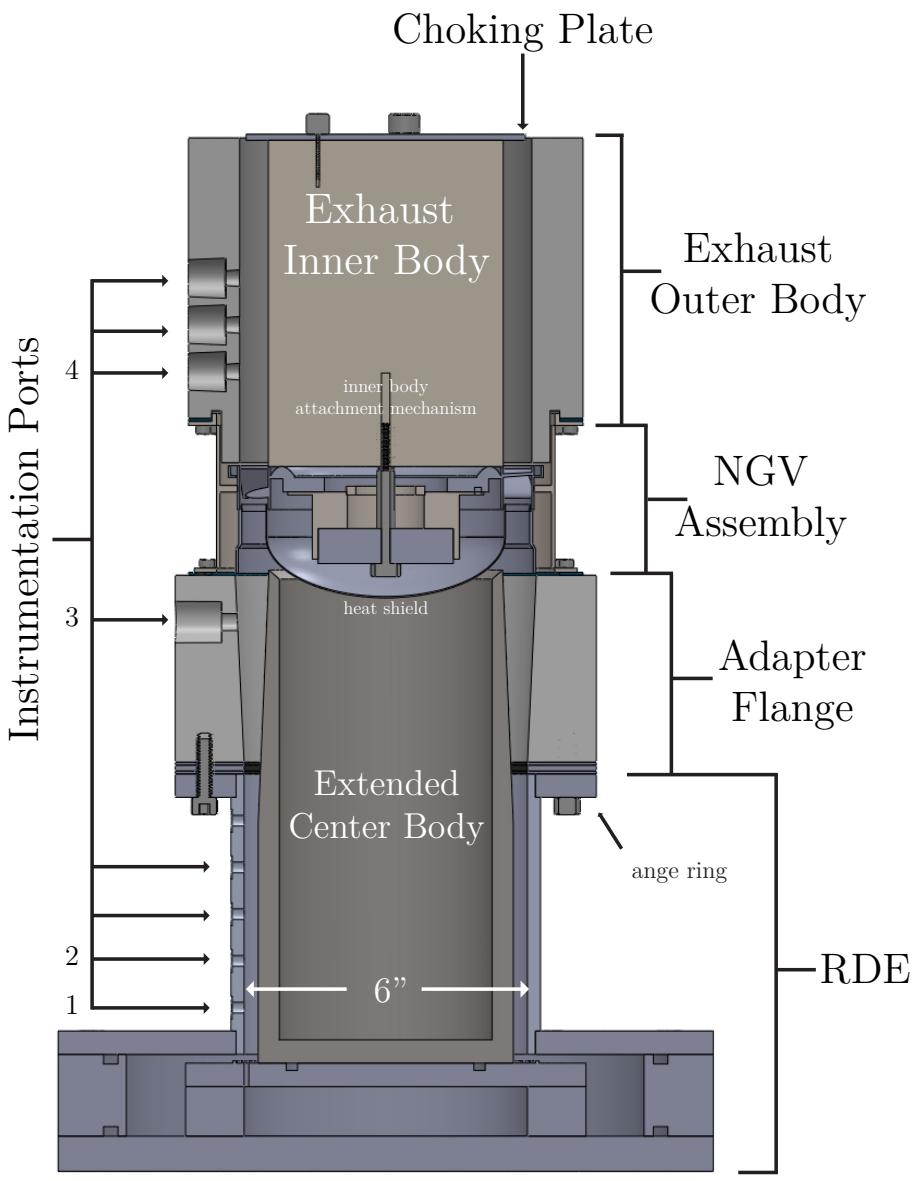

Figure 3.6. Complete RDE/integration/NGV assembly

3.3.0.1 Corrected Mass Flow.

To determine if the six inch RDE and the T63 NGV components are a suitable match, the corrected mass flow ($\dot{m}_c$) for the RDE was calculated and compared to the T63 $\dot{m}_c$ using Eq. (3.1). Corrected mass flow is a useful metric because it accounts for differences

in operating conditions for each component to allow for meaningful comparison. A total temperature of $T_t = 3700$ °R at an equivalence ratio of $\phi = 0.4$ and a mass flow of $\dot{m} = 2.98$ and a total pressure of $P_t = 95$ psia was measured in the RDE. T63 operational documentation [14] provides required variables including a mass flow of $\dot{m} = 2.679 \frac{lbm}{sec}$ at a $T_{t_4} = 2298.5$ °R, and a $P_{t_4} = 77.614$ psia. P_{std} for Wright-Patterson Air Force Base is 14.25 psi. This yields an agreeable pairing of corrected mass flows, with the RDE corrected mass flow of $\dot{m}_c = 1.01 \frac{lbm}{sec}$ and the T63 corrected mass flow of $\dot{m}_c = 1.07 \frac{lbm}{sec}$.

$$\dot{m}_c = \dot{m} \frac{\sqrt{\frac{T_t}{T_{std}}}}{\frac{P_t}{P_{std}}} \tag{3.1}$$

3.3.0.2 Extended RDE Center Body.

The extended RDE center body, shown in Fig. 3.7, extends the standard RDE center body up and tapers to the heat shield on the bottom of the NGV assembly. This maintains the axial and azimuthal flow path of the RDE exhaust and reduces turbulent unsteady mixing prior to entering the NGV assembly. The RDE exhaust flows in the annulus between the adapter flange and the extended RDE center body into the nozzle guide vanes.

3.3.0.3 Adapter Flange.

The adapter flange, shown in Fig. 3.8, directs the RDE exhaust into the NGVs via a slight increase in area to accommodate the NGV inlet radius. The RDE exit flow is channeled into the same flow path that the gas turbine T63 combustor air would follow. Geometry of this piece is such that there are no discontinuities or step geometry changes. The adapter flange has three instrumentation ports spaced 120° apart to allow access to the flow prior to entering the NGVs.

(a) Extended RDE center body

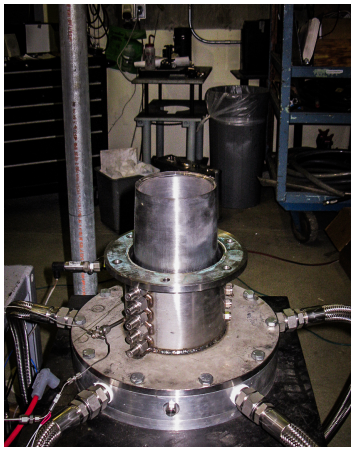

(b) Setup with 6” RDE and extended RDE center body

Figure 3.7. RDE extended center body installation

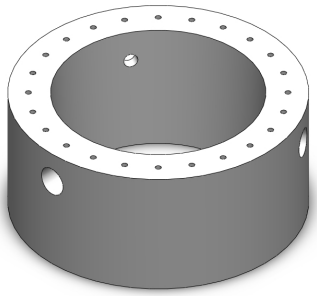

(a) Adapter Flange

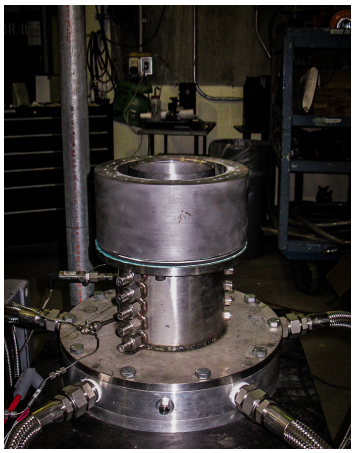

(b) Setup with 6” RDE, extended RDE center body, and adapter flange

Figure 3.8. Adapter flange installation

3.3.0.4 Exhaust Inner Body.

The exhaust inner body, shown in Fig. 3.9, is simply a large steel cylinder with the purpose of maintaining an annulus flow path at the NGV exit. The inner body prevents turbulent mixing at the NGV exit plane so that measurements are representative of the actual exhaust flow. The exhaust inner body is tapped with three holes on the top for securing a choking plate that is sized to choke the NGV exit flow at RDE operational mass flows.

3.3.0.5 Exhaust Outer Body.

The exhaust outer body, shown in Fig. 3.10, constrains the NGV exit flow to allow for instrumentation and meaningful data acquisition. The outer body has three axially spaced sets of three access ports spaced 120° apart for instrumentation access as well as a single instrumentation port between one of the three-port sets. A detailed drawing of these ports is found in Appendix A. The outer body is designed to fit into the T63 NGV assembly.

(a) Exhaust inner body

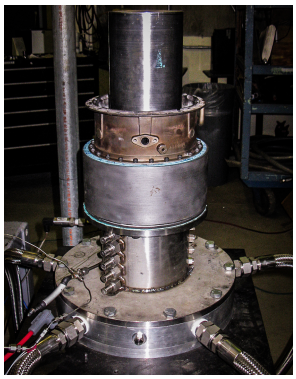

(b) Setup with 6" RDE, extended RDE center body, adapter flange, NGV assembly, and exhaust inner body

Figure 3.9. T63 NGV assembly and exhaust inner body installation

(a) Exhaust outer body

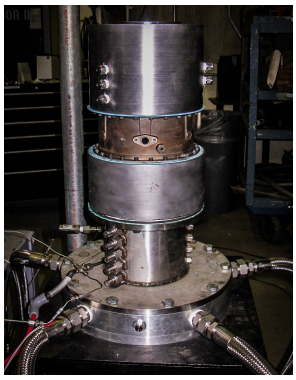

(b) Setup with 6" RDE, extended RDE center body, adapter flange, NGV assembly, and exhaust inner/outer bodies

Figure 3.10. Exhaust outer body installation

3.4 Successful Run Criteria

For this study to be effective, the RDE must actually detonate. At each equivalence ratio and mass flow test point, PCB® high speed dynamic pressure data was used to verify detonation similar to methods used by Shank [9]. That is, a quick and useful estimation of the detonation speed was accomplished by checking the PCB® data seen in Fig. 3.11 in the control room. A simple calculation involving the time between peaks and the RDE circumference allows the operator to determine if detonation speeds have been reached. Reasonable average detonation speeds, calculated from NASA's Chemical Equilibrium with Applications program (CEA), range from 1480 to 1700 m/s for equivalence ratios between 0.4 and 0.55. The time between peaks and corresponding detonation speed shown on the figure is an example of the variation in detonation speed from one peak to another, as the average detonation speed for the entire run was 1700 m/s. The upper-left inset of Fig. 3.11 shows the thermal drift due to high heat loads, evidenced by the decreasing zero of the

pressure spikes. High-speed video footage, which is normally used to determine presence of detonation, was not practical as the view of the detonation channel is blocked by all of the downstream components.

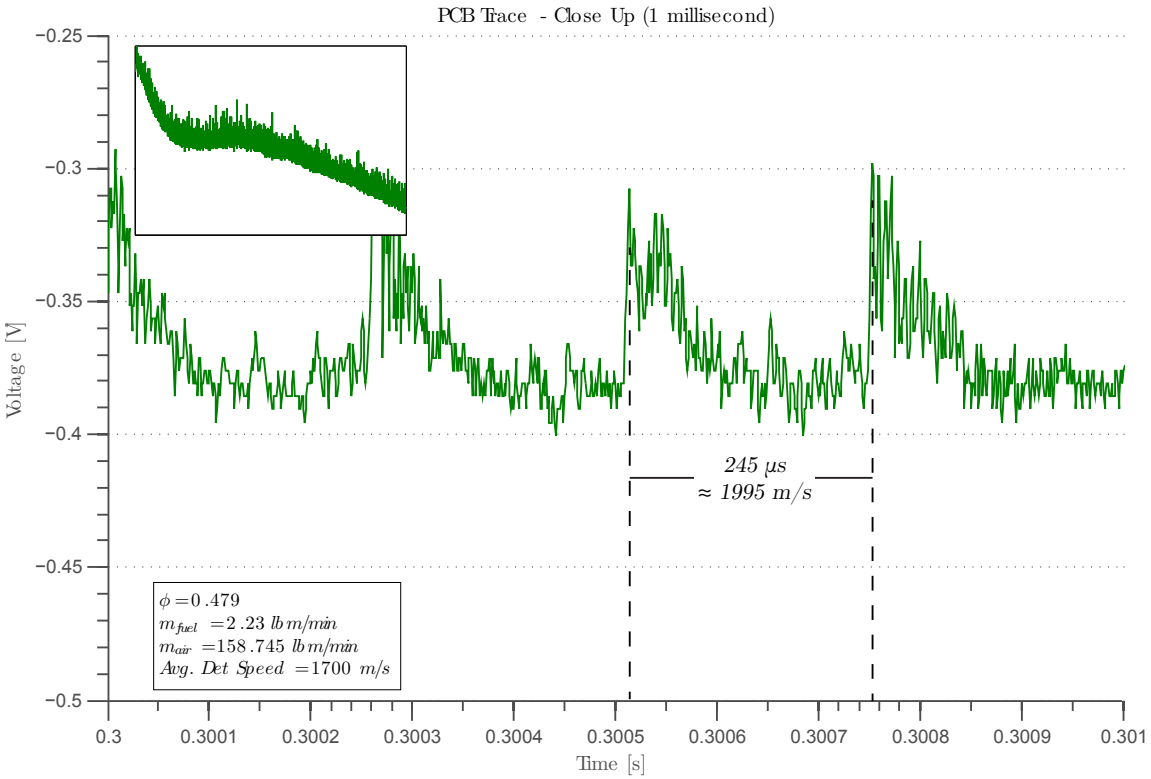

Figure 3.11. High-speed PCB® trace used to assess successful detonation

3.5 Instrumentation

The RDE and NGV integration assembly are designed for flexibility in type and location of instrumentation. The entire setup contains multiple sets of 120° offset instrumentation ports, shown previously in Fig. 3.6. Several types of probes and transducers were used to acquire data sets during this study. Locations of interest for instrumentation were the detonation channel of the RDE and the instrumentation ports upstream and downstream of the NGVs. In Fig. 3.6, port 2 was used for instrumentation in the detonation channel, port 3

was used for instrumentation upstream of the NGVs, and port 4 was used for instrumentation downstream of the NGVs.

Time between detonation wave pressure peaks is determined by a PCB® 112A05 piezoelectric transducer located in instrumentation port 3. The PCB® measures dynamic pressure with a response time of less than 1 μs and shows the peak voltage each time the detonation wave passes. Based on the circumference of the 6 in RDE and an estimated V_{CJ} of 1950 m/s, the detonation wave has an expected frequency of about 4 kHz with a peak-to-peak time of 246 μs. With rise times of less than 1 μs, the pressure transducer will not miss a pressure spike. However, the transducer records pressures to within 1% of the range of the 5000 psi sensor for an accuracy of ±50 psi. Shank [9] and Russo [11] found that detonation front pressures recorded by the pressure transducer are between 300 and 500 psi. It follows that this large ±50 psi bias error renders the actual pressure measurements useless. Rather, it is the time of each individual pressure peak that is of importance to this study. The high frequency dynamic pressure data from the transducer is recorded by the data collection computer in the control room at 2 MHz. While thermal drift precludes gathering meaningful dynamic pressures, the peak voltages allow for the calculation of detonation wave speed via dividing the circumference of the RDE channel by the time between peak voltages. One dynamic pressure transducer was placed in the detonation channel of the RDE at instrumentation port 2, a second dynamic pressure transducer was placed in an adapter flange at instrumentation port 3 upstream of the NGVs, and a third dynamic pressure transducer was placed in the exhaust outer body at instrumentation port 4, downstream of the NGVs. This arrangement of dynamic pressure probes allows for monitoring of the detonation pressure peaks and describes the attenuation of these pressure peaks as the flow moves through the adapter flange and NGVs.

Stagnation pressure upstream and downstream the NGVs was measured with a pitot probe manufactured at D-Bay by placing a 90 degree bend in $\frac{1}{16}$ inch diameter stainless

steel tubing after a 5 in lead. The pitot probe was connected to a Capillary Time Averaged Pressure (CTAP) setup in which the pitot lead connects to a $\frac{1}{16}$ in diameter tube with a length of 3 ft. An Omegadyne® PX429-250A5V pressure transducer was attached at the end of this 3 ft length of tubing. Attenuation through the 3 ft tube dampens instantaneous fluctuations and provides time averaged pressure readings. The pitot probes were placed at the same planar locations as the dynamic pressure probes. The CTAP rise time dictated the need for single test run times of at least $\frac{1}{2}$ second.

Temperature data was acquired with the use of an Omega® KMQSS-062E-6 k-type exposed bead thermocouple. The thermocouple uses dissimilar metals which generate a small voltage which is calibrated to yield a temperature. The exposed 0.038 in diameter bead thermocouple was used in an effort to decrease the rise time of the thermocouple, as a grounded k-type thermocouple did not approach a final value within the one second run time at which the RDE operates. The thermocouple was placed in the assembly at instrumentation port 3 to provide temperature upstream the NGVs.

3.6 Data Reduction

This study utilized data reduction techniques previously developed and validated by Shank [9] and Russo [11]. PCB® data was analyzed with a time-of-flight code developed by Russo [11]. This MATLAB® code, found in Appendix B, determines the location and time between pressure peaks in the instantaneous PCB® data. With the time between peaks and the RDE geometry, the code uses Eq. 3.2 to find the detonation velocity. The reader is referred to Russo [11] for greater detail in the validation and sensitivity study of the time-of-flight code.

$$V_{det} = \frac{\text{combustion channel circumference}}{\text{time between pressure peaks}} \tag{3.2}$$

Following Russo's development and validation of the time-of-flight code, Shank [9] made changes to the code that reflects differences in testing geometry. Because Shank's

geometry was used in this study, his changes to the data reduction code were also used. The first change is in the hold time. The code determines an average pressure for the entire data set and then looks for peaks that are more than one standard deviation above the average. After finding the peak, the code enacts a hold time during which the peak searches are suspended. This stops the code from counting the same peak twice. In accordance with the previously mentioned expectation of V_{CJ} of 1950 m/s and detonation frequency of 4 kHz, the code was altered to have a hold time of 240 μs.

Another change made by Shank that was used in this study is a refinement of the criteria for a peak. Russo's original code required 4 data points to lie at least one standard deviation above the mean for a peak to be counted and resulted in a calculation of a two velocity bands - one at subsonic deflagration speeds and another at detonation speeds. Shank [9] reduced the required number of points to 2 resulting in the removal of the subsonic velocity band. This change was validated through high-speed video analysis.

IV. Results and Discussion

This study was an investigation of RDE exhaust flow through the NGV section of a T63 gas turbine engine. The study was primarily concerned with the unsteadiness of the flow upstream and downstream of the NGVs and the total pressure drop over the NGVs. A number of thermocouple tests were also completed to acquire an approximate temperature of the flow upstream and downstream of the NGVs. The study utilized Shank's [9] previously developed RDE with a known operational space. Successful detonations were determined via analysis of time between instantaneous pressure peaks which yielded the detonation velocity. From previous work by Shank [9], detonation velocities for this RDE running on hydrogen and air were expected to be 1400 to 1600 m/s.

4.1 Initial Testing

The first test run with the integration assembly design yielded successful detonation but highlighted a design flaw and the need for an improved fastener design for the exhaust inner body. This test had no instrumentation, and was run with standard air (21% O_2) and H_2. The thin $\frac{1}{8}$ in washer used to secure the exhaust inner body was replaced with a $\frac{3}{4}$ in thick disk, to which bolts were welded to prevent rotation of the inner body via insertion into pre-existing oil channel holes in the T63 NGV assembly. Also, the $\frac{3}{8}$ in bolt securing the exhaust inner body was replaced with a $\frac{1}{2}$ bolt, and a lock washer was added to prevent spin. The new setup was tested at an equivalence ratio of 0.964 and a successful 1 s run was completed with air and fuel mass flows of 161 $\frac{lbm}{min}$ and 4.57 $\frac{lbm}{min}$, respectively. Figure 4.1 shows a frame of the standard speed 30 fps video during the detonation. It is believed that the sparks from the exhaust are bits of metal from the heat shield which endured great vibrational stress during testing.

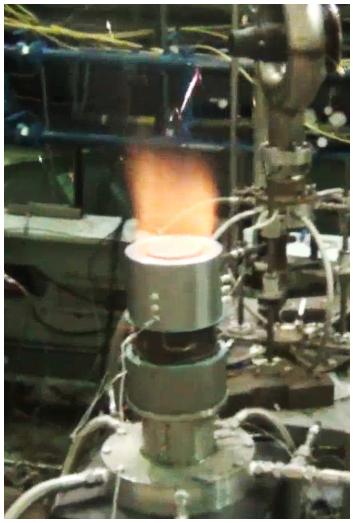

Figure 4.1. Early test of the RDE with the NGV assembly

4.2 Detonation Wave Speed

Detonation wave speeds in this study, with an average of 1672 m/s, were consistently on par with those seen in a previous study by Shank [9] using the same RDE. Each individual run was analyzed with the previously mentioned time-of-flight code, to include a detonation wave speed calculation, as well as histograms and moving average plots that show the variability of the wave speed within any given run, shown in Fig. 4.2 and Fig. 4.3.

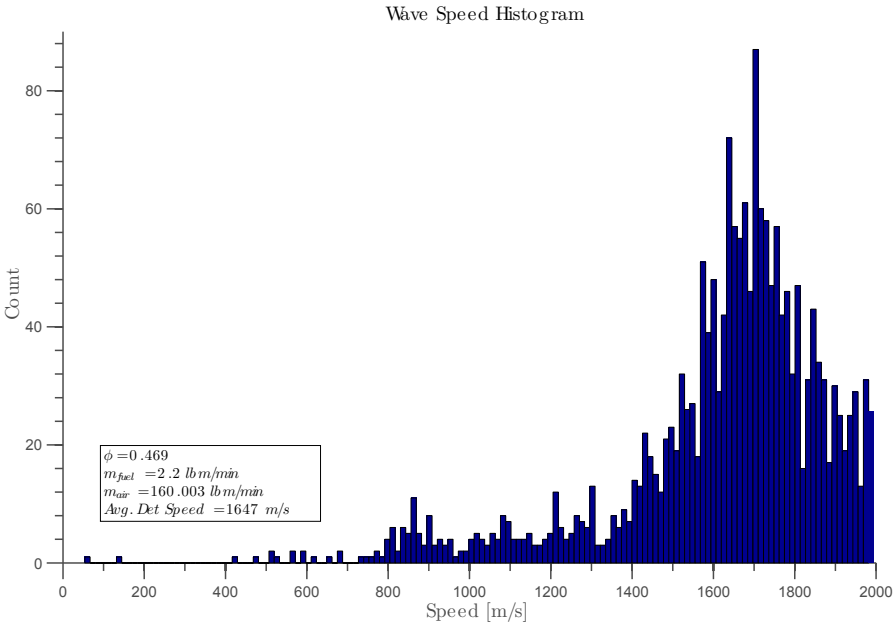

Figure 4.2. Histogram detonation wave speeds for a single run

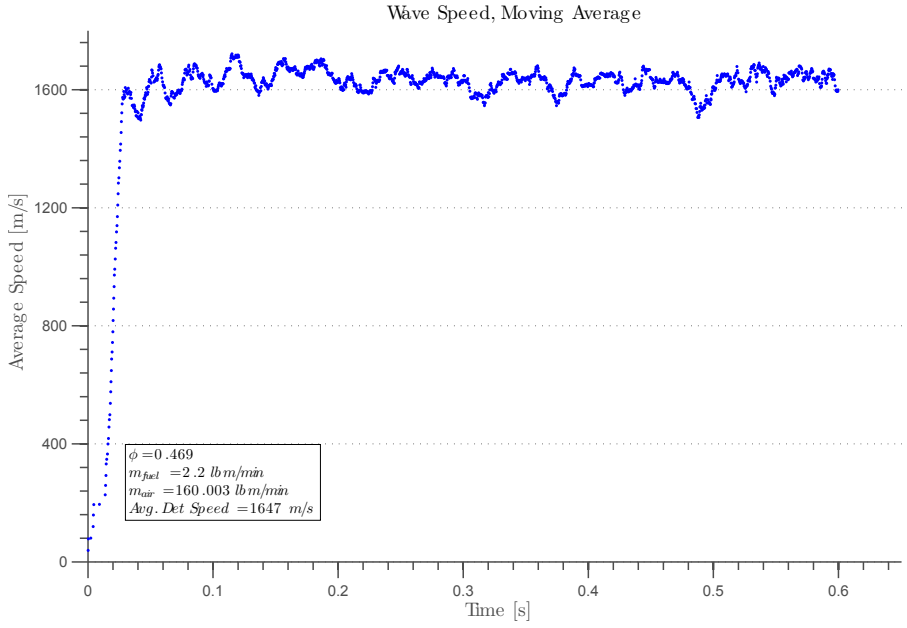

Figure 4.3. Detonation speed moving average for a single run

View of an actual PCB® dynamic pressure transducer trace provides further confirmation of detonation. Figure 4.4 shows the entire set of transducer voltage traces in the detonation channel and upstream and downstream of the NGVs. This overall view of the pressure traces allows us to see the characteristic thermal drift which is often caused by high heat transfer, evidenced by the downward slope of the traces. This high heat transfer is often a good sign of successful detonation.

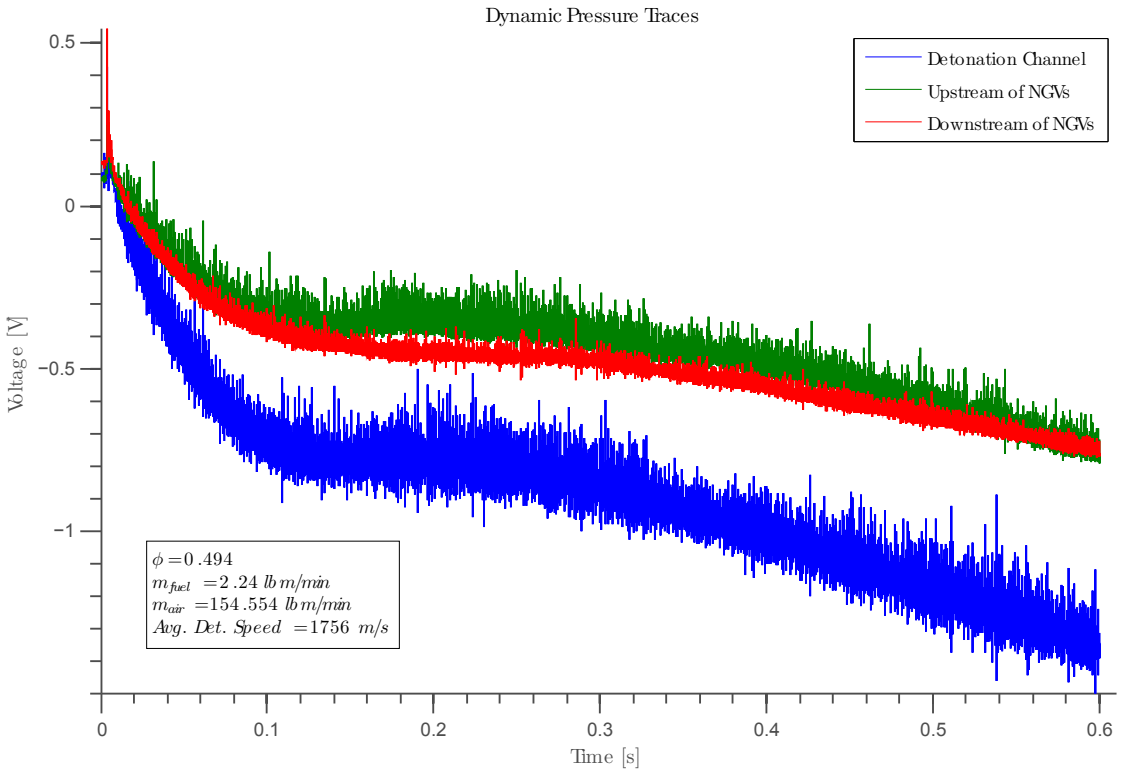

Figure 4.4. Dynamic pressure traces of an entire 0.5 s run with $\dot{m}_{total} = 162.203\ \frac{lbm}{min}$ and $\phi = 0.469$

A closer look at the pressure traces, shown previously in Fig. 3.11 and below in Fig. 4.5, provides a view of the actual pressure peaks due to detonation. The transducer immediately upstream of the NGVs allows for the best determination of detonation wave speed. The

pressure transducer in the detonation channel, which is normally used for detonation wave speed calculations, had irregularities where pressure peaks were not as clearly defined, especially when compared to signals from prior research by Shank [9]. This irregular signal is likely due to complicated flow structures caused by the presence of downstream components that were not present in previous studies. Notably, possible shocks caused by the heat shield and NGVs are a likely cause of this transducer trace structure. The dynamic pressure transducer trace upstream of the NGVs in instrumentation port 3 provides a cleaner signal with measurable peaks that does in fact correspond to expected detonation wave speeds. The time between detonation pressure peaks changes, shown in Fig. 4.3, and reflects the variable nature of the detonation wave speed throughout the run.

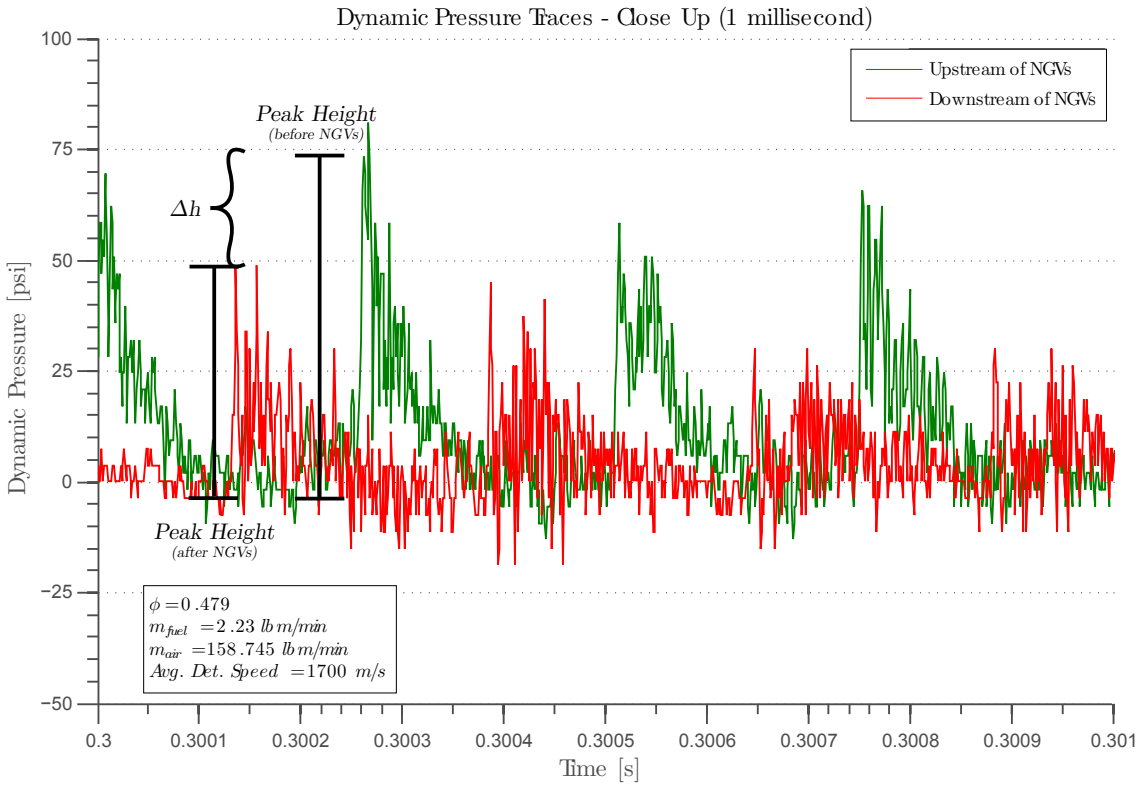

Figure 4.5. PCB® trace of 1 millisecond from a 0.5 s run

Finally, the PCB® data was analyzed with a Fast Fourier Transform (FFT) algorithm. FFT converts the signal into magnitude and phase components of each frequency. The final product is a spectrum of frequencies present in the input signal, as seen in Fig. 4.6. By using the circumference of the RDE it is possible to compute the detonation wave speed corresponding to the prominent frequency shown in the FFT plot. The rightmost frequency spike in Fig. 4.6 is believed to correspond to a harmonic resonance of the setup.

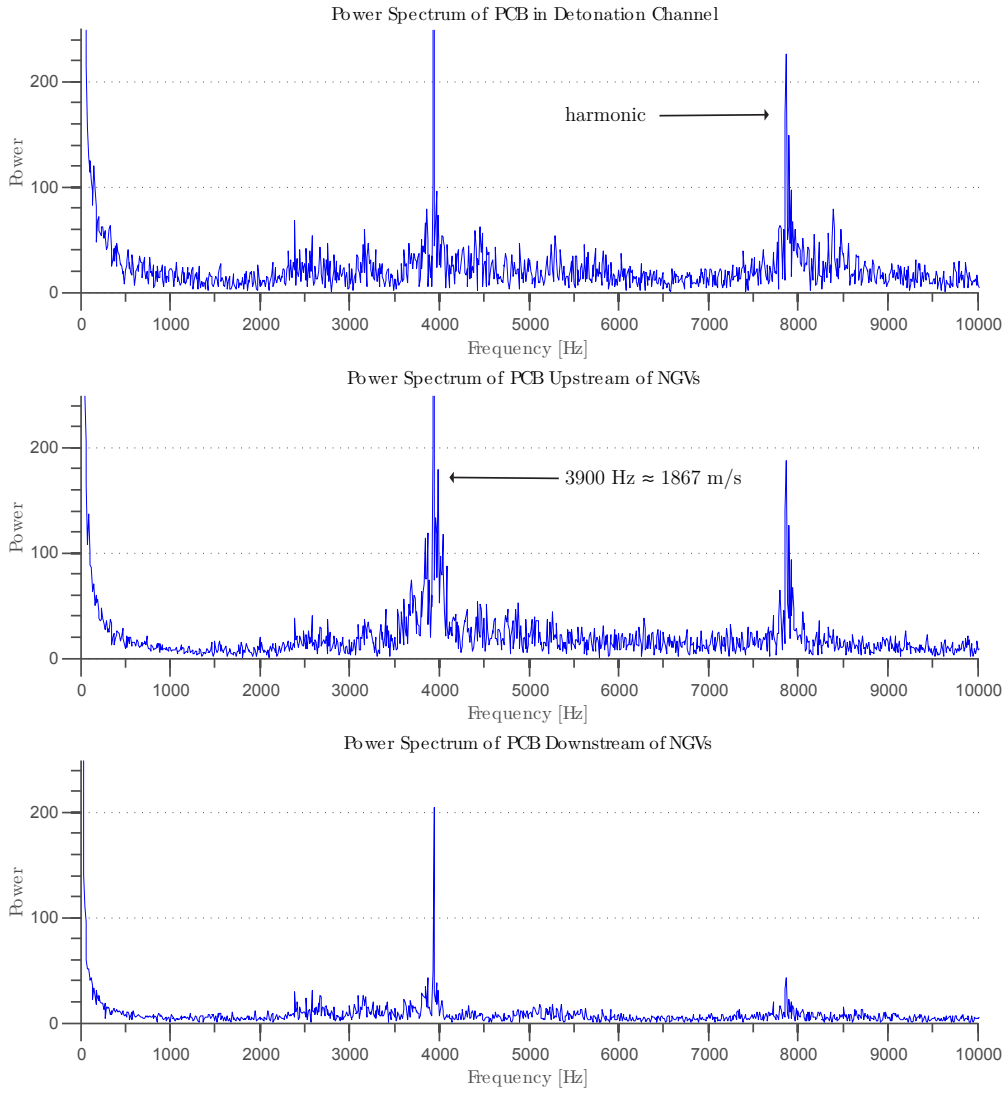

Figure 4.6. Frequency plots for PCB® data throughout the flow assembly

The values found for detonation speed as a function of equivalence ratio are shown in Fig. 4.7. The trend of increasing detonation wave speed as equivalence ratio increases is consistent with previous research by Shank [9] and Russo [11].

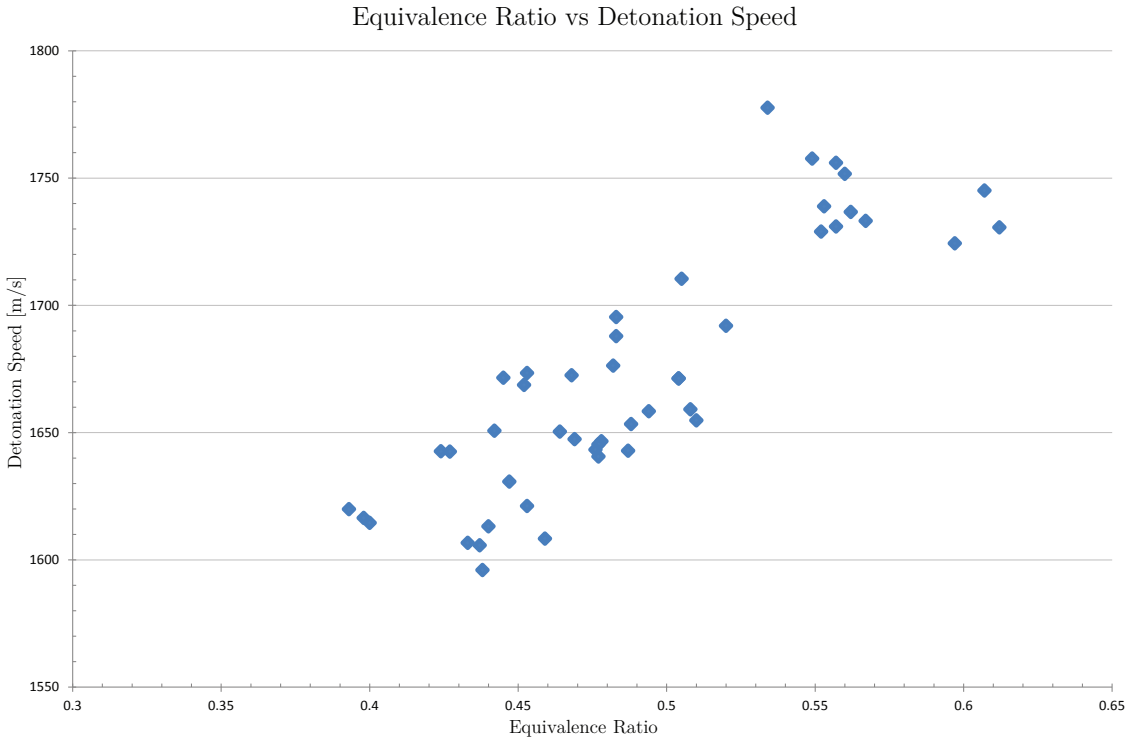

Figure 4.7. Detonation wave speed as a function of equivalence ratio

4.3 Unsteadiness

Of great interest to this study was the unsteadiness of the flow upstream and downstream of the NGVs. The instantaneous nature of the dynamic pressure transducer data provides not only a measure of detonation wave speed but also a metric for evaluating unsteadiness of the flow. To use this metric, the author developed a MATLAB® code similar to the time-of-flight code. The code sweeps through the dynamic pressure transducer data in search of pressure spikes indicating a detonation. The code records the dynamic pressure value at the spike,

and then sweeps before and after the point for a local minimum pressure. An example of the peak height is shown in Fig. 4.5. With this data the dynamic pressure detonation peak heights are found without being skewed by the thermal drift inherent in the data. An average detonation peak height was calculated for each dynamic pressure trace for each run and the percent change of these values upstream and downstream of the NGVs was used as the metric to evaluate change in unsteadiness.

In all cases, the unsteadiness of the flow was attenuated through the NGVs, with a 60% average decrease over 46 individual tests. Figure 4.8 shows that there is no clear correlation between total mass flow and unsteadiness of the flow. It was also found that neither equivalence ratio nor detonation wave speed have a clear correlation to unsteadiness decrease. The unsteadiness decrease varies between 56% and 64%.

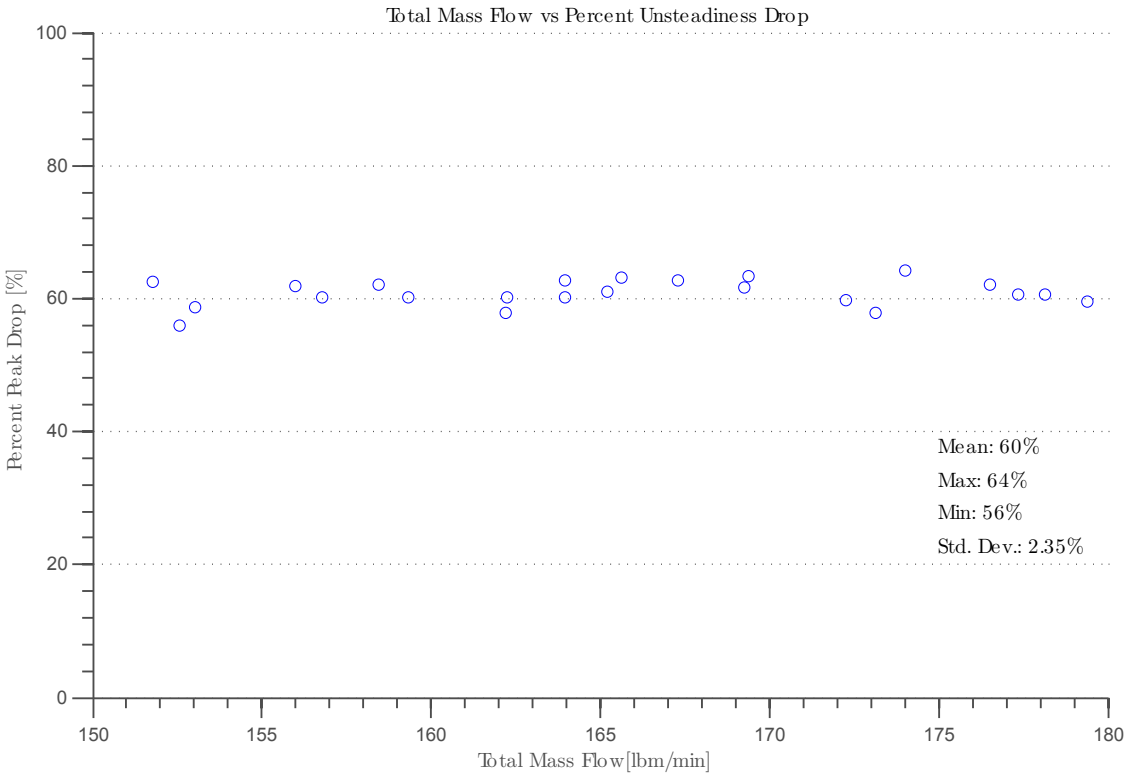

Figure 4.8. Unsteadiness as a function of total mass flow

4.4 Temperature

An added interest in characterizing the flow path of the RDE exhaust through the NGV assembly was determining the temperature of the flow.Using the K-type exposed bead thermocouple located in instrumentation port 3 upstream of the NGVs revealed the exhaust gases to be approximately 2250 R. Figure 4.9 shows the thermocouple trace upstream of the NGVs in instrumentation port 3 during a 1 s run at an equivalence ratio of $\phi = 0.41$. Run time was lengthened to 1 second from the normal 0.5 seconds to allow for the rise time of the thermocouple. This test was repeated 3 times to ensure fidelity of the data.

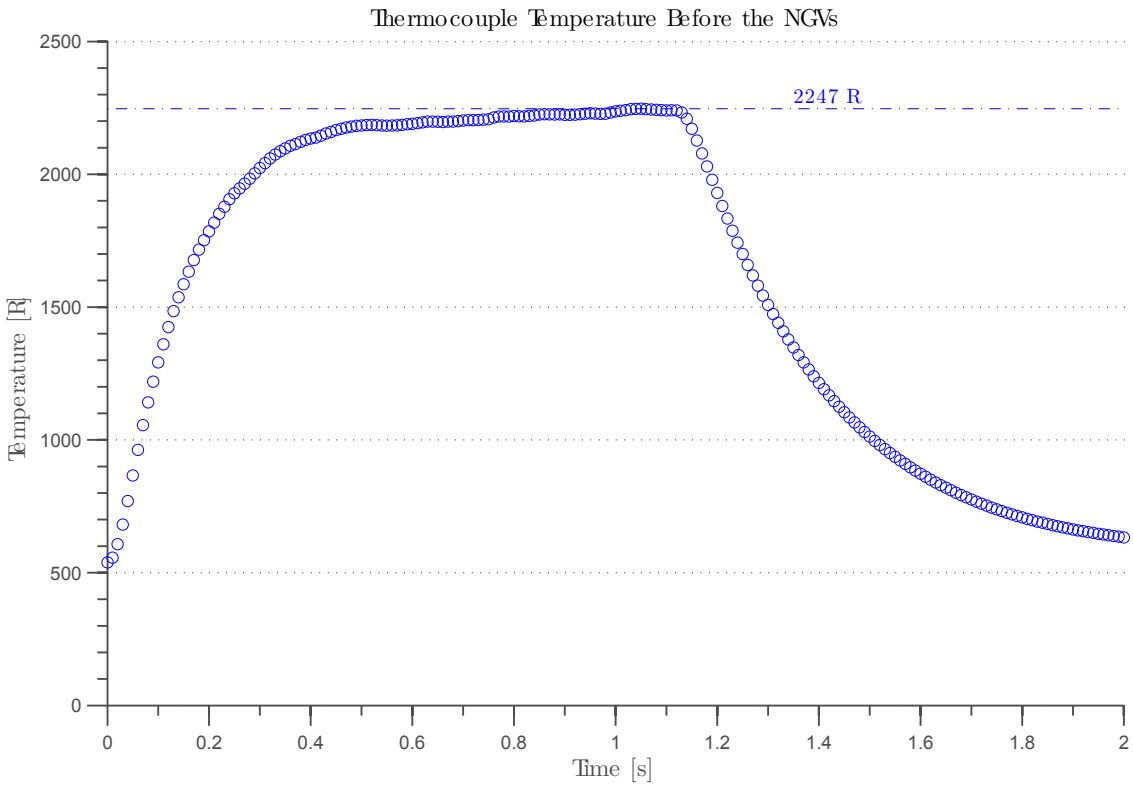

Figure 4.9. Temperature upstream of the NGVs

Using this temperature of 2247 °R, a total pressure of $P_t = 90$ psia (taken from data presented in the following subsection), and Eq. 3.1, the corrected mass flow was $\dot{m}_c = 1.01$

$\frac{lbm}{sec}$. This corrected mass flow matches well with the corrected mass flow of the T63, which is approximately $\dot{m}_c = 1.07\ \frac{lbm}{sec}$.

4.5 Stagnation Pressure

Stagnation pressure upstream and downstream of the NGVs is the final measurement of interest in this study. By measuring stagnation pressure it is possible to not only determine the percent total pressure drop across the NGVs but also gain a rough idea of the flow direction as it exits the NGVs by orienting a pitot probe at varying angles in the flow, shown in Fig. 4.10.

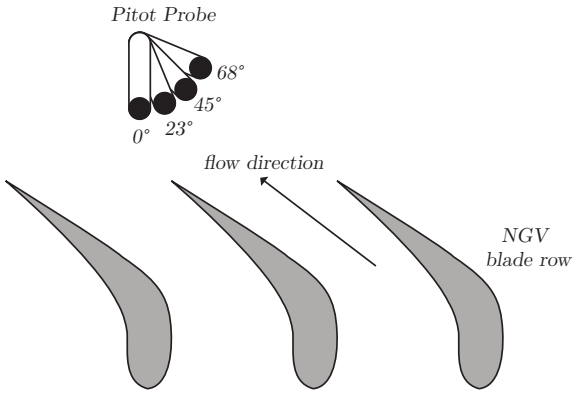

Figure 4.10. Pitot probe angles in NGV flow

Measuring accurate stagnation pressure requires that the pitot probe is oriented roughly directly into the flow. The NGVs were estimated to have an exit angle of approximately 60° from physical blade measurements. Twenty-two test runs at an equivalence ratio of 0.45 ±0.05 and total mass flow of 165 ±7 $\frac{lbm}{min}$ were accomplished in which the pitot probe downstream of the NGVs was oriented at 0°(straight down), 23°, 45°, and 68°, shown in Fig. 4.10. Figure 4.11 shows that the pitot probe pressure readings were highest around 45° and 68° which indicates the flow angle is somewhere between 40° and 55°.

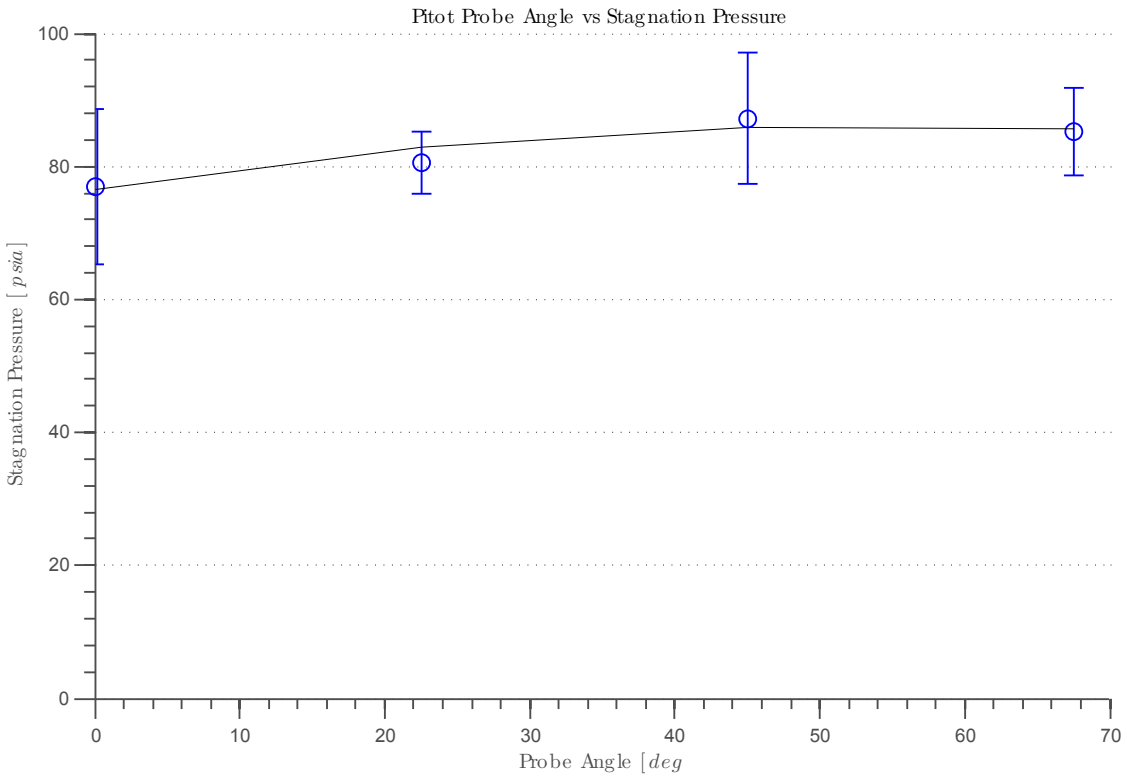

Figure 4.11. Variation in pitot probe stagnation pressure due to changes in pitot probe orientation

After determining optimal orientation of the pitot probe in the NGV exhaust flow it was possible to compare stagnation pressures upstream and downstream of the NGVs and determine percent total pressure drop. Figure 4.12 shows the percent pressure decreases for six test runs of varying equivalence ratio and total mass flow with a downstream pitot probe orientations of 45° and 68°, and an upstream pitot probe orientation of 0°. There is no noticeable correlation between mass flow and percent pressure drop, nor is there a correlation between equivalence ratio or detonation speed and percent pressure drop. The average percent decrease in this configuration was 4%. This value correlates to the 5% stagnation pressure drop seen in the T63 gas turbine engine during ongoing research at AFRL.The flow upstream of the NGVs at instrumentation port is approximately M = 0.138,

which can be calculated using the effective area of the NGVs of A = 3.02 in^2 and the exit area of the adapter flange/extended RDE center body of A = 12.9383 in^2.

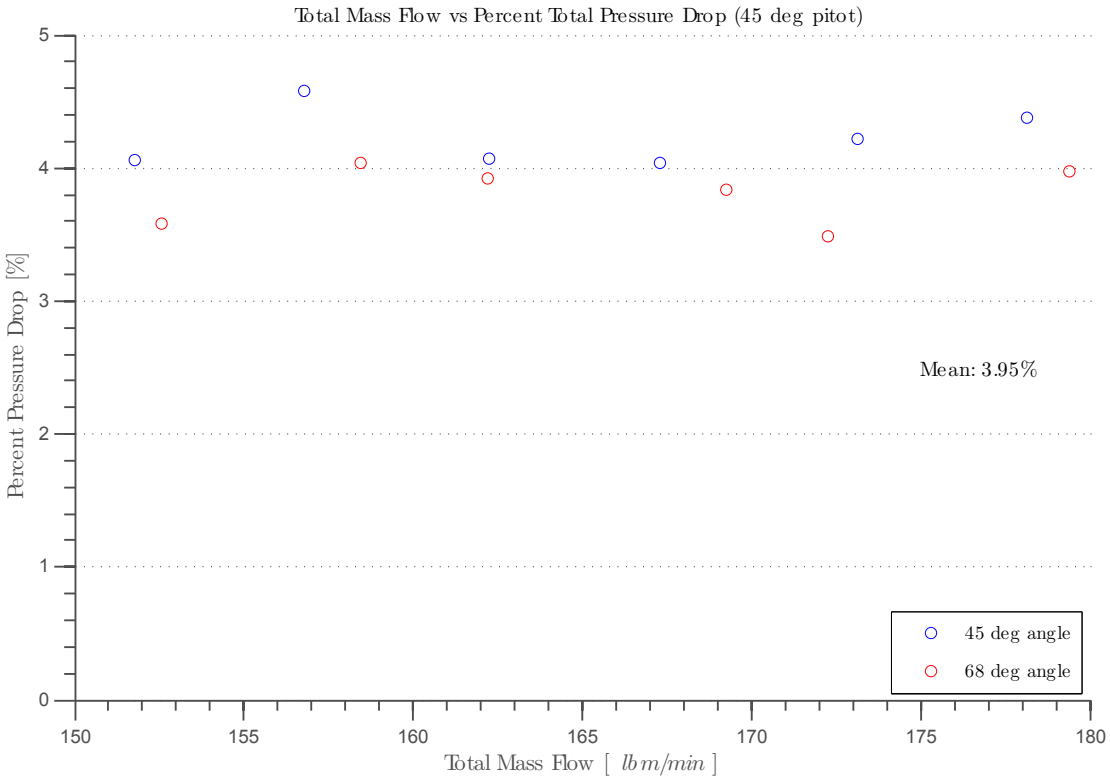

Figure 4.12. Percent stagnation pressure decrease upstream and downstream of NGVs

V. Conclusions and Recommendations

This study focused on advancing the experimental and developmental understanding of rotating detonation engines in regards to integration with turbomachinery. The goal of the study was to design integration hardware to attach and instrument a set of T63 NGVs to the exhaust of an RDE and then characterize the flow through the NGVs by measuring unsteadiness and pressure.

5.1 Conclusions

The integration design was comprised of an extended RDE center body, an adapter flange, and exhaust inner and outer bodies. These parts are shown in Figs. 3.7 to 3.10. The design directed the RDE exhaust through the NGVs with minimal discontinuities and attempted to maintain the azimuthal and axial flow directions of the exhaust.

The use of both a smaller fuel plate spacer as well as a back pressure plate allowed for successful detonation at equivalence ratios lower than those seen in previous studies. Instantaneous dynamic pressure signals were noisier in the RDE channel than upstream of the NGVs, and the less-noisy signal from upstream of the NGVs was used for detonation velocity calculations. Detonation velocities were similar to those found in previous studies by Shank [9] with an average of 1672 m/s. Unsteadiness decreased by an average of 60% over the NGVs. This unsteadiness, measured as the attenuation of peak height in the instantaneous dynamic pressure signals, was not correlated to equivalence ratio, mass flow, or detonation speed.

Temperature of the RDE exhaust approximately 10 in axially downstream of the detonation front was approximately 2250 °R.

Pitot probe angle sweeps in the NGV exhaust flow indicate a flow angle somewhere between 40° and 55° as compared to a metal blade exit angle of roughly 62°. Percent

stagnation pressure decrease over the NGVs was an average of 4.22%. It was found that this pressure drop is not correlated to equivalence ratio, mass flow, or detonation velocity.

5.2 Recommendations

This study is an initial step for integrating RDEs into the flow path of gas turbine engines. A closer look at NGV exhaust flow angle could be accomplished via a wedge directional probe with a short lead to allow for instantaneous readings. This would also provide more insight into the unsteadiness of the flow downstream of the NGVs. Actual visual characterization of the NGV exhaust flow would be possible with a side view quartz exhaust outer body to view the swirl induced by the NGVs.

There are issues in RDE operation that have yet to be solved that greatly impact this study. Most notably, the various modes of operation cited by Shank [9] of rotation, reversal, and bifurcation cause great variability in the RDE exhaust flow. Additionally, detonation waves in the RDE do not consistently travel in the same direction. A study for acquiring consistent, unidirectional detonation waves would be useful prior to integrating turbomachinery into the exhaust flow.

Appendix A: Integration Assembly Schematics

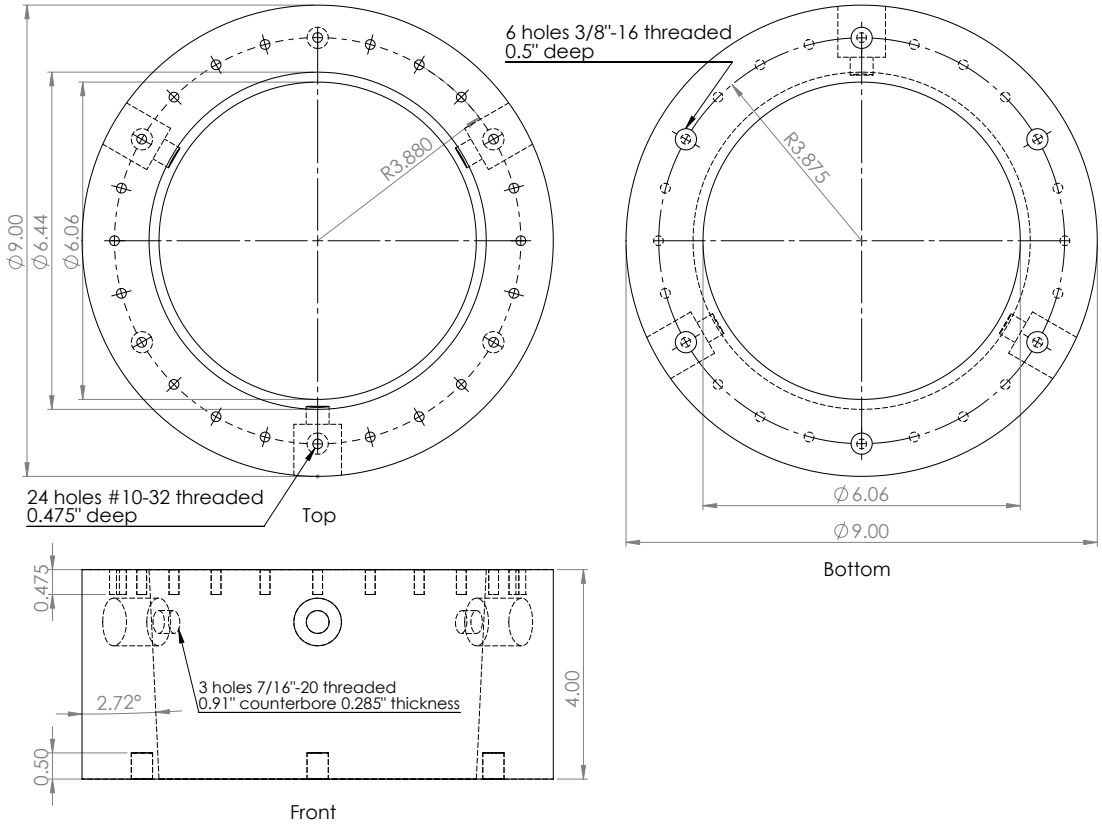

Figure A.1. Adapter Flange Schematic

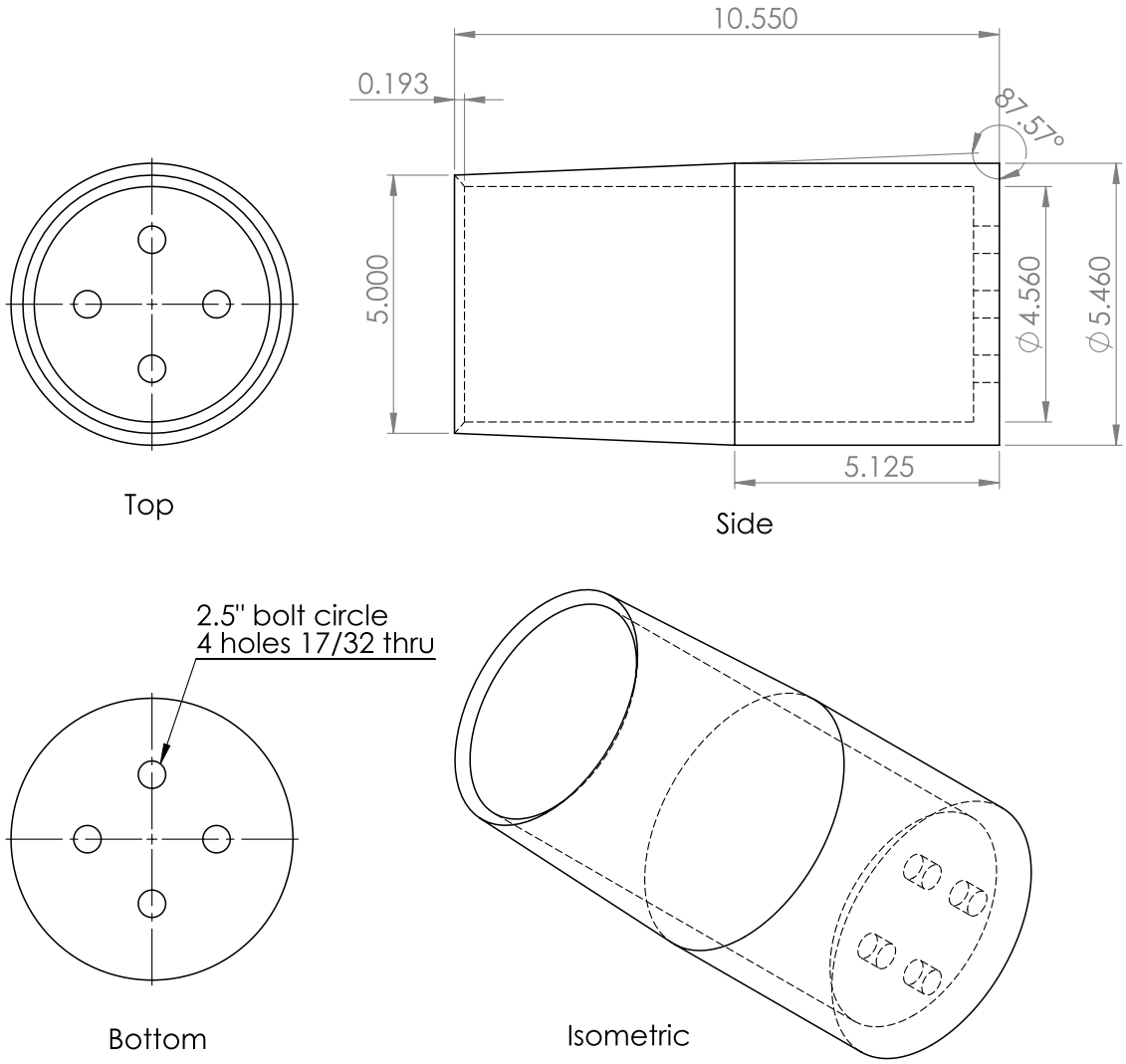

Figure A.2. RDE Extended Center Body Schematic

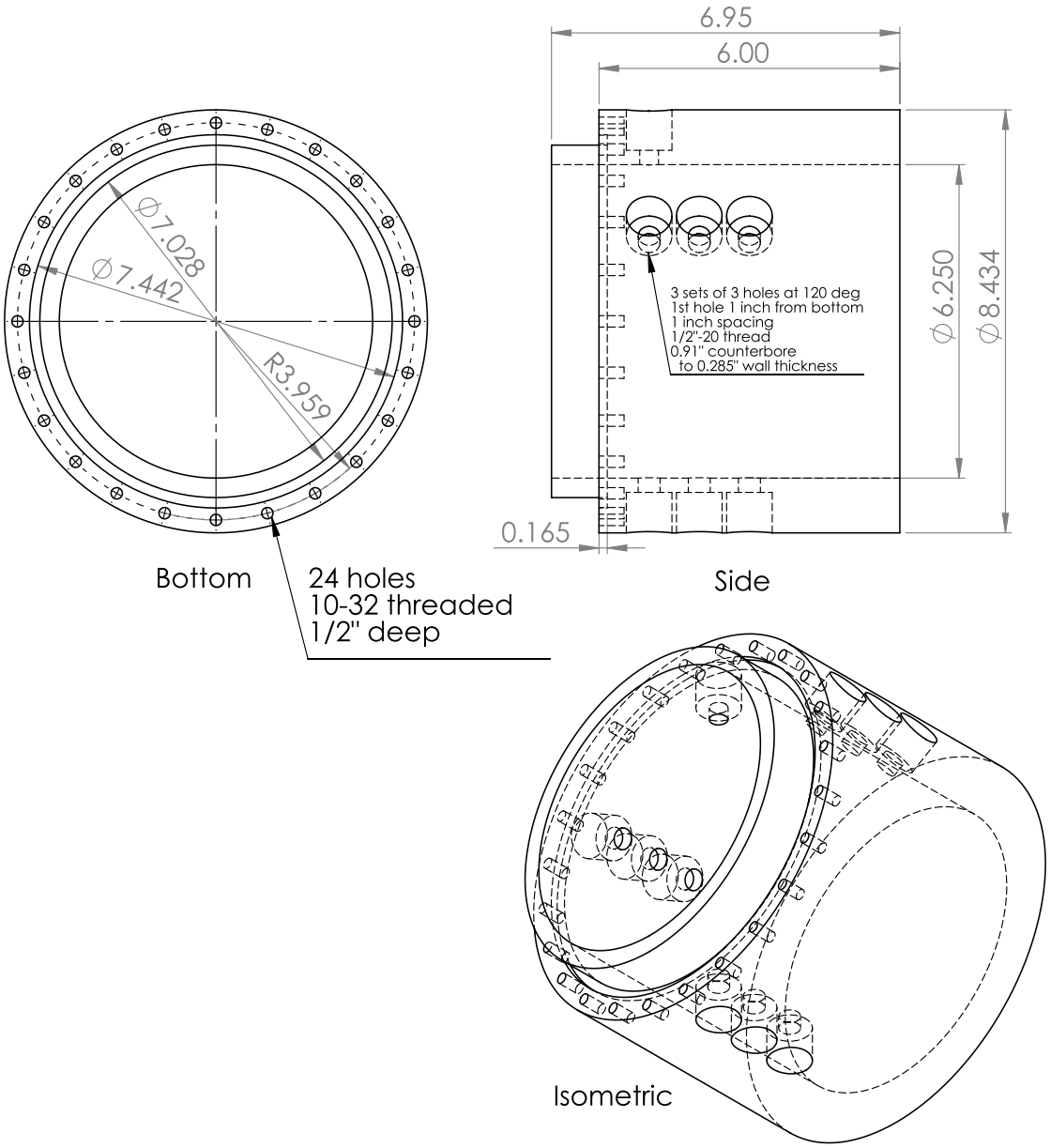

Figure A.3. Exhaust Outer Body Schematic

Appendix B: Time of Flight Code

This code was written and validated by Russo [11]. Shank [9] altered Russo's [11] original code to modify the hold time and criteria for a pressure peak.

```
function [wsTime,waveSpeed,blah,err_bias_diam,err_bias_t1,err_bias_t2,...
    err_bias,avg_detSpeed,percent_err] = time_of_flight(data,chan,dist)
%[time,speed] = test(data,chan,dist)
%
% Test calculates time of flight wave speed for a single PCB pressure ducer in
% a RDE channel and returns a vector of waves speeds and their associated run
% times. Wave detection is based on the ion probe drop algoritm used in
% PTFinder.
%
% Input: data - row array of pressure data. First row must be time.
% chan - channel to calculate wave speed from
% dist - circumference of channel (0.47877872 meters for 6" RDE)
%
% Output: time - vector of times of each speed measurement
% speed - vector of wave speeds
close all
% Extract time and signal from the array
time = data(1,:);
trace = data(chan+1,:);
% Calculate a moving average, and a threshold
a=1;
b=ones(1001,1)./1001;
avg = filter(b,a,trace);
stdev = std(detrend(trace,'linear',(1000:3000:999999)'));
thresh = (avg+stdev);
```

```
% Setup looping variables
ind = find(trace > thresh); % indices of data points above threshold
ctr = 0; % point counter
passes =[0 0 0 0]; % indices of wave passes
iPass = 1; % current wave pass number
latch = false; % logical variable for preventing false triggers
% loop through data points above threshold
for i = 1:length(ind)-1
% ignore data within 240us of a wave pass
if latch
if (time(ind(i))-time(passes(iPass-1))) > 240e-6
else
continue
end
end
% check for a set of two points in a row
if ind(i) == ind(i+1)-1
% increment the counter if points are adjacent
ctr = ctr+1;
else
% reset the counter if not
ctr = 0;
end %if
% Record the time and begin ignoring data when a wave pass is detected
if ctr >= 2
passes(iPass) = ind(i-1); % time of wave pass
iPass = iPass+1; % keep track of the current wave pass
latch = true; % set a logical to ignore data for the next 60us
ctr = 0; % reset the counter for the next pass
end %if
end %for i
% Calculate times and wave speeds
```

```
wsTime = (time(passes(1:end-1))'+time(passes(2:end))')/2; % average of two passes
waveSpeed = dist./diff(time(passes)'); % change in time over circumfrence
figure
plot(wsTime,waveSpeed,'.')
xlabel('Time (s)')
ylabel('Speed (m/s)')
title('Wave Speed')
avgspeed=mean(waveSpeed);
stdev_vel=std(waveSpeed);
blah=1;
for iii=1:length(waveSpeed)
if waveSpeed(iii)<1000
combustSpeed=zeros(iii);
combustSpeed(blah)=waveSpeed(iii);
blah=blah+1;
end
end
avg_combustSpeed=mean(combustSpeed);
blah=1;
for iii=1:length(waveSpeed)
if (waveSpeed(iii)>1000 && waveSpeed(iii)<1960);
detSpeed(blah)=waveSpeed(iii);
blah=blah+1;
end
end
avg_detSpeed=mean(detSpeed);
mode_detSpeed=mode(detSpeed);
speed_ratio=avg_combustSpeed/avg_detSpeed;
b = ones(51,1)./51;
waveSpeed_avg=filter(b,a,waveSpeed);
figure
plot(wsTime,waveSpeed_avg,'.')
```

```
xlabel('Time (s)')
ylabel('Average Speed (m/s)')
title('Wave Speed, Moving Average')
figure
hist(waveSpeed,150)
xlabel('Velocity (m/s)')
blah=diff(time(passes)'); %delta t (sec)
err_bias_diam=(3.141592654*.000127)./blah'; %know diam to .005 in
%know time to .5 micro sec
err_bias_t1=(dist*(.5*10^-6))./((time(passes(1:end-1))).^2);
%know time to .5 micro sec
err_bias_t2=(-dist*(.5*10^-6))./((time(passes(2:end))).^2);
err_bias=(err_bias_diam.^2+err_bias_t1.^2+err_bias_t2.^2).^.5;
err_bias_use=mean(err_bias);
%for 95% confidence interval, from p185 of Intro to Engineering Experimentation
err_precision=2*stdev_vel;
err_tot=(err_bias_use^2+err_precision^2)^.5;
percent_err=(err_tot/avgspeed)*100;
```

Appendix C: Data Points

Average Wave Speed [m/s]	Equivalence Ratio	Total Mass Flow [lbm/min]
1606	0.45	176.54
1613	0.51	156.00
1620	0.48	163.97
1617	0.48	165.23
1615	0.48	165.65
1695	0.45	174.03
1673	0.44	177.34
1688	0.46	169.38
1669	0.48	163.94
1673	0.49	159.32
1692	0.51	153.03
1752	0.51	151.76
1756	0.49	156.79
1731	0.48	162.24
1778	0.46	167.28
1758	0.45	173.14
1739	0.43	178.13
1729	0.42	179.39
1731	0.44	172.26
1737	0.43	169.25
1733	0.47	162.20
1724	0.49	158.46
1745	0.50	152.58
1672	0.45	176.54
1710	0.51	156.00

Average Wave Speed	Equivalence Ratio	Total Mass Flow
1676	0.48	163.97
1647	0.48	165.23
1645	0.48	165.65
1621	0.45	174.03
1596	0.44	177.34
1608	0.46	169.38
1643	0.48	163.94
1653	0.49	159.32
1659	0.51	153.03
1655	0.51	151.76
1658	0.49	156.79
1641	0.48	162.24
1650	0.46	167.28
1631	0.45	173.14
1643	0.43	178.13
1643	0.42	179.39
1651	0.44	172.26
1607	0.43	169.25
1647	0.47	162.20
1643	0.49	158.46
1671	0.50	152.58

Bibliography

[1] Nordeen, C.A. and D. Schwer. Divergence and Mixing in a Rotating Detonation Engine. *51st Aerospace Sciences Meeting*, Jan 2013. AIAA 2013-1175.

[2] Voitsekhovskii, B.V., Mitrofanov, V.V., and M.E. Topchian. Investigation of the Structure of Detonation Waves in Gases. *Symposium (International) on Combustion*, 12:829–837, 1969.

[3] Bykovskii, Fedor A., Zhdan, Sergey A., and Evgenii F. Vedernikov. Continuous Spin Detonations. *Journal of Propulsion and Power*, 22:1204–1216, Nov 2006.

[4] Bussing, T. and G. Pappas. An Introduction to Pulse Detonation Engines. *32nd Aeropsace Sciences Meeting and Exhibit*, January 1994. AIAA 94-0263.

[5] Lee, John S. *The Detonation Phenomenon*. Cambridge University Press, New York, NY, 2008.

[6] Chapman, D.L. On the Rate of Explosion of Gases. *Philosophical Magazine*, 45, 1899.

[7] Dremin, Anatoly N. *Toward Detonation Theory*. Springer, New York, NY, 1999.

[8] Zeldovich, Y.B. The Theory of the Propogation of Detonation in Gaseous Systems. *Experimental and Theoretical Physics*, 10:542, 1940.

[9] Shank, Jason R. Development and Testing of a Rotating Detonation Engine Run on Hydrogen and Air. Master's thesis, Graduate School of Engineering and Management, Air Force Institute of Technology (AU), Wright-Patterson AFB OH, March 2012. AFIT/GAE/ENY/12-M36.

[10] Kailasanath, K., and D.A. Schwer. Rotating Detonation Engine Research at NRL. International Workshop on Detonation for Propulsion, September 2012. Washington, DC.

[11] Russo, Rachel M. Operational Characteristics of a Rotating Detonation Engine Using Hydrogen and Air. Master's thesis, Graduate School of Engineering and Management, Air Force Institute of Technology (AU), Wright-Patterson AFB OH, March 2011. AFIT/GAE/ENY/11-J03.

[12] Tellefsen, Jonathan R. Build Up and Operation of an Axial Turbine Driven by a Rotary Detonation Engine. Master's thesis, Graduate School of Engineering and Management, Air Force Institute of Technology (AU), Wright-Patterson AFB OH, March 2012. AFIT/GAE/ENY/12-M39.

[13] Naples, A., et. al. Flowfield Characterization of a Rotating Detonation Engine. *51st Aerospace Sciences Meeting*, January 2013. AIAA 2013-0278.

[14] Allison Engine Company. *Allison 250 Series II Training Manual*. Rolls-Royce Aerospace Group, 1996.

REPORT DOCUMENTATION PAGE

Form Approved
OMB No. 0704–0188

1. REPORT DATE *(DD–MM–YYYY)*	2. REPORT TYPE	3. DATES COVERED *(From — To)*
21–03–2013	Master's Thesis	Oct 2010–Mar 2012

4. TITLE AND SUBTITLE

Characterization of Rotating Detonation Engine Exhaust Through Nozzle Guide Vanes

5a. CONTRACT NUMBER

5b. GRANT NUMBER

5c. PROGRAM ELEMENT NUMBER

6. AUTHOR(S)

DeBarmore, Nick D., Second Lieutenant, USAF

5d. PROJECT NUMBER

5e. TASK NUMBER

5f. WORK UNIT NUMBER

7. PERFORMING ORGANIZATION NAME(S) AND ADDRESS(ES)

Air Force Institute of Technology
Graduate School of Engineering and Management (AFIT/EN)
2950 Hobson Way
WPAFB, OH 45433-7765

8. PERFORMING ORGANIZATION REPORT NUMBER

AFIT-ENY-13-M-09

9. SPONSORING / MONITORING AGENCY NAME(S) AND ADDRESS(ES)

Intentionally Left Blank

10. SPONSOR/MONITOR'S ACRONYM(S)

11. SPONSOR/MONITOR'S REPORT NUMBER(S)

12. DISTRIBUTION / AVAILABILITY STATEMENT

DISTRIBUTION STATEMENT A:
APPROVED FOR PUBLIC RELEASE; DISTRIBUTION UNLIMITED

13. SUPPLEMENTARY NOTES

14. ABSTRACT

A RDE has higher thermal efficiencies in comparison to its traditional gas turbine counterparts. Thus, as budgets decrease and fuel costs increase, RDEs have become a research focus for the United States Air Force. An integration assembly for attaching the first NGV section from a T63 gas turbine engine to a 6 inch diameter RDE was designed and built for this study. Pressure, temperature, and unsteadiness measurements were completed in this study to characterize the exhaust flow of the RDE through the NGVs. The experiment found that stagnation pressure dropped an average of 4% through the NGVs, and that unsteadiness as a measurement of dynamic pressure trace peak height was attenuated by a mean of 60% across the NGVs. Additionally, the study found the flow angle of the NGV exhaust to be between 40° and 55°. Finally, the study found that the RDE exhaust flow was approximately 2250 °R before entering the NGVs.

15. SUBJECT TERMS

RDE rotating detonation engine turbine NGV turbomachinery integration

16. SECURITY CLASSIFICATION OF:			17. LIMITATION OF ABSTRACT	18. NUMBER OF PAGES	19a. NAME OF RESPONSIBLE PERSON
a. REPORT	b. ABSTRACT	c. THIS PAGE			Dr. Paul I. King (ENY)
U	U	U	UU	63	19b. TELEPHONE NUMBER *(include area code)* (937) 255-3636 x4628 paul.king@afit.edu